Republic of Iraq
Ministry of Higher Education & Scientific Research
University of Technology
Building and Construction Engineering Department

ESTABLISHMENT OF 3D MODEL WITH

Digital Non-Metric Camera

in Close Range Photogrammetry

A THESIS SUBMITTED TO THE
A DEPARTMENT OF BUILDING AND CONSTRUCTION ENGINEERING,
UNIVERSITY OF TECHNOLOGY,
IN PARTIAL
FULFILLMENT OF THE REQUIREMENTS FOR THE DEGREE OF
MASTER
OF SCIENCE IN BUILDING AND CONSTRUCTION ENGINEERING
(*Geomatics Engineering*)

By

Aysar jameel Aljanabi

B. Sc., (Surveying Engineering) 1999

Supervised by

Assist. Prof. Dr. Abbas Zedan Khalaf

Supervised by

Dr. Imzahim Abdulkareem Alwan

2012

بسم الله الرحمن الرحيم

قَدْ جَاءَكُمْ بَصَائِرُ مِنْ رَبِّكُمْ فَمَنْ أَبْصَرَ فَلِنَفْسِهِ وَمَنْ عَمِيَ فَعَلَيْهَا وَمَا أَنَا عَلَيْكُمْ بِحَفِيظٍ

صدق الله العلي العظيم

الانعام (١٠٤)

To

My Family

With love and respect

CERTIFICATION

We certify that this thesis entitled **"Establishment of 3D Model With Digital Non-Metric Camera in Close Range Photogrammetry"**, was prepared by **Aysar Jameel Aljanabi**, under our supervision at the Building and Construction Engineering Department of the University of Technology, in a partial fulfillment of the requirements for the degree of Master of Science in Geomatics Engineering.

Signature:

Name: ***Assist. Prof. Dr.*** **Abbas Zedan Khalaf**
(Supervisor)
Date: / / 2012

Signature: Imzahim

Name: ***Lecturer Dr.*** **Imzahim Abdul kareem Alwan**
(Supervisor)
Date: / / 2012

In view of the available recommendations, I foreword this thesis for debate by Examining Committee

Signature
Dr. **Abbas Zedan Khalaf**
Head of
Geomatics Engineering Branch
Date: 29/ 1 1/ 2012

COMMITTEE CERTIFICATION

We certify that we have read this thesis entitled, **"Establishment of 3D Model With Digital Non-Metric Camera in Close Range Photogrammetry"**, and as Examining Committee examined the student **Aysar Jameel Aljanabi** in its content and in what is connected with it and in our opinion it meets the standard of a thesis for the degree of Master of Science in Civil Engineering (Geomatics Engineering).

Signature:
Assist. Prof. Dr. **Abbas Zedan Khalaf**
(Supervisor)
Date: 29 / 11 / 2012

Signature: Imzahim
Lecturer Dr. **Imzahim Abdul kareem Alwan**
(Supervisor)
Date: / / 2012

Signature:
Assist. Prof. Dr. **Alaa S. Mahdi**
(Member)
Date: 29 / 11 / 2012

Signature: Khalid
Senior Sci. Res. Dr. **Khalid Ibrahim Hassoon**
(Member)
Date: / / 2012

Signature:
Name: ***Prof. Dr.*** **Abdul_Razzak T. Ziboon**
(Chairman)
Date: / / 2012

Signature: Riyad Alanbari
Prof. Dr. **Riyad Hassan Al-Anbari**
The Head of
Building and Construction Engineering Department
Date: / / 2012

ACKNOWLEDGEMENTS

All profusion praise and thanks be to Allah for his uncountable help and strength which he gave me to achieve this work.

Throughout the period of my research, I have benefited greatly from the guidance, advice and sympathy of teachers, colleagues and friends, to all of whom I wish to offer my warmest thanks. I would like to express my gratitude and deep thanks to my supervisors **Assist. Pof. Dr. Abbas Zedan Kalaf**, and Dr**. Imzahim Abdulkareem Alwan** for their supervision, guidance, constructive criticism and encouragement through this work.

I would also like to thank my family for always being there with their encouragement, prayer and patience.

I would like also to express my gratitude to all the staff of the Geomatics Engineering in the Department of Building and Construction ,University of Technology for their support and help.

I would like to express my gratefulness and deep thanks to **Mr. Bashar Saleem Abbas** for his guidances, for support and help through this work..

Aysar

Abstract

The basic data source of 3D modeling of regular or irregular surfaced objects are known (or calculated) point coordinates. Obtaining 3D model of the irregular surfaced objects need plenty of points to represent the surface exactly. These points can be easily obtained both traditionnal methods and from the measurement of the photographs.

This study is achieved in three stages. The first stage the calibration of camera.Two cameras have been used in this study; NIKON COOLPIX AW100, and SANYO E1075. They were calibrated in two different focal lengths, five times for each camera. The results obtained were varying in focal length (c) and (x_p , y_p) the coordinates of the center of projection of the image (principal point), the difference was ranged (0.02 - 0.04) mm. It could be considered as big compared to the proposed accuracy of photogrammetry. So, to obtain a high accuracy from close range photogrammetry, the camera must be calibrated in the field without shutting down the camera is an important matter.

The second stage is the production of 3D object in cloud points dependind on the sampling rate and taking many captures. In this case, an object of face-shaped clay was used and a 3D object is performed with (5563) 3D points with sampling rate (1 mm). The smaller sampling rate results in longer processing and more points. This case could be beneficial in documentation of cultural and historical heritage in a digital library in observing the variation with time.

Photomodeler Scanner (version 6) program software was used in the last stage as a measuring tool for a sample of small house. There were two cases of

measuring the sides of such house, the first case used coded targets were defined automatically to the program. These targets were fixed on the sides of the sample. The accuracy of measurement was high, ranging from (10) to (30) micrometer. The second case measures without coded targets, the points defined manually using mouse to referencing points in images and production of a 3D points to measure a distance between points, the accuracy from this case was about (0.1) to (0.5) mm. A photomodeler needs to include any knwon distance beteewn two points on the object to the photomodeler software, and then the program will calculate the three dimensional coordinates to any point.

An image of building located in the University of Babylon was taken as a final case of the study. The image was 25 m. distance from the camera. The building was represented in 3D model with tremendous number of points about (53715) points and the standard error in calibrating the coordinates was $\delta x = \mp 0.057 mm., \delta y = \mp 0.11 mm., \delta z = \mp 0.33 mm.$

Contents

List of Tables

List of Figures

LIST OF ABBREVIATIONS

3D……..……...……Three dimensional

2D……..……..Two dimensional

I.O.P……Interior Orientation Parameter

E.O.P…….……..……Exterior orientation Parameter

XL,YL,ZL = (Xo , Yo , Zo)……The Ground coordinates of the camera station

v……..…….……Residuals

w……Weight matrix

B……..Matrix of partial derivatives with respect to the unknowns

Δ……Vector of corrections

N, t……....Normal equations matrices

f……..Vector of evaluated observations with approximate unknown

ω……...Rotation angle around the x axis

φ……Rotation angle around the y axis

κ……Rotation angle around the z axis

m's……..Elements of rotation matrix

c……..Focal length

I……..Identity matrix

B^e ……...Matrix of partial derivatives with respect to the (e.o.) parameters

B^s…….Matrix of partial derivatives with respect to the ground coordinates

Δ^e……Vector of corrections to the (e.o.) parameters

Δ^s……...…….Vector of corrections to the ground coordinates

Δ^i……..Vector of corrections to the additional parameters

w^e……Weight matrix of the (e.o.) parameters

w^s…….……Weight matrix of the ground coordinates

GCi…….……Ground Coordinates of point i

PhCi……Photo Coordinates of point i

APs……...……Additional Parameters

w^i……..Weight matrix of the additional parameters

CCD…….……..Charge Coupled Device

RMS……Root Mean Square

CHAPTER ONE

INTRODUCTION

1.1 INTRODUCTION

Today, three dimensional (3D) models were used in a wide away of fields. The medical industry uses detailed models of organs. The movie industry uses them as characters and objects for animated and real life motion pictures. The architecture industry uses them to demonstrate proposed buildings and landscapes. The engineering community uses them as designs of new devices, vehicles and structures as well as a host of other uses. The use of three dimensional computer graphics and visualization techniques is becoming more and more popular, because these techniques visualize more realistic object models than graphic based object models. However, in most applications of 3D modeling and visualization, large and complex 3D models data are required.

The term Photogrammetry means the process of measuring images on a photograph. An integrated digital Photogrammetry system is defined as hardware/software configuration that produces photogrammetric products from digital imagery using manual and automatic techniques. Nowadays, there is an increasing demand for full three dimensional data of planning, architecture, archaeology, environmental analysis, civil engineering, tourism, computer animation, historical preservation, mechanical inspection, and ship construction [1].

To depict the real condition of the object, and to measure 3D of all the corners of the structure, particularly the inaccessible points, creation of accurate 3D models are very much necessary. Recent years have seen a number of developments in geometric modeling of historical monuments in 3D, especially their structural details and textures [2].

Close Range Photogrammetry is a measurement technology that can be used for the extraction of 3D points from the photographs; further, these points are useful for the accurate 3D modeling and visualization. Digital Photogrammetry derives all the appropriate measurements from the photographs itself rather than measurements directly from the objects. Due to the digital data flow, photogrammetry has now become an efficient alternative to the classical building measurement and reconstruction methods [3]. This thesis discusses the various 3D model generation techniques and shows the advantages of photogrammetry techniques for measurements. For the present project, an experiment has been conducted to check the accuracy of the 3D model generated using the photogrammetric technique.

The complete orientation and calibration is done automatically or manually based on the photographs only. The objects selected are the artificial object face-shaped, made of clay, a small model of building and building located in the University of Babylon. In this research, there are two cameras used: Nikon Coolpix AW100, and SANYO E1075. The processing is done using photogrammetric software package Photomodeler Scanner (version 6).

The tradition of any research in Photogrammetry, we need a known control point to complete the project. In this thesis, there is another approach to work with photogrammetry is Photomodeler software. In such approach, it needs to include any known distance between two points in the object to the Photomodeler software, and then the program will calculate the three dimensional coordinates to any point on the object, as well as the distance between any two points, area and size.

1.2 Literature Review

Substantial work has been done during the past years to obtain a 3D model from two or more photographs, documentation of the cultural heritage, monitoring and measurements using close range photogrammetry with photogrammetric software package Photomodeler.

To understand the performed work more clearly, some of the selected previous works can be summarized as follows:

Heuvel (1998) [4] explained that the study deployed setups that require at least two photographs to obtain dimensional information in three-dimensions (3D). This requires a large number of control points to correlate the photographs. The data obtained are used to create computer models from the photographs. Methodologies for the use of single images have been used to obtain both two-dimensional (2D) and 3D geometry from the images when applying constraints such as straight lines and vanishing points.

Gomes (1999) [5] presented the results of an architectural photogrammetric project using the PhotoModeler software. The results showed that with comparison to the conventional photogrammetric procedure, PhotoModeler allows even greater reduction of time and costs for the production of models, since it does not require positioning and measuring of targets and stereoscopy to produce suitable photographic documents.

Guidi and Tucci (2001) [6] described the activity reported as a recent experiment in 3D scanning of a highly complex sculpture: the wooden statue "Maddalena" by Donatello, kept in the museum of the "Opera

del Duomo", in Florence. The acquisitions, taken with a commercial system based on fringe projection, give a local measurement uncertainty of about 70µm, but when the complete model is generated by automatic alignment of the raw 3D images in a common coordinate system, possible scale variations might be involved, especially along the height of the statue. With this preliminary work, the authors want to verify the metric reliability of the three-dimensional model, obtained through iterative alignments of single 3D acquisitions.

Lara and Tyler (2004) [7] presented a paper focusing on the role of PhotoModeler close range Photogrammetry software package, an important facet of traffic accident reconstruction-vehicle crash measurement. More specifically, this study applied the PhotoModeler process to control crash information generated by the National Highway Traffic Safety Administration (NHTSA). A statistical technique known as bootstrapping was utilized to generate distributions from which the variance was examined. The "within" subject analysis showed that 44.8% of the variability is due to the technique itself and the "between" subjects analysis demonstrated that 55.2% of the variability is attributable to vehicle type-roughly half and half. Additionally, a 95% CI for the "within" analysis revealed that the mean difference (between this study and NHTSA) fell between -2.52 mph and +2.73 mph; the "between" analysis showed a mean difference between -3.26 mph and +2.41 mph.

Low-cost digital cameras have shown the potential for use in close-range digital photogrammetric measurements after lens calibrations is preformed. Chandler (2005) [8] presented an experimental test model out medium density fiberboard and a reference digital elevation model (DEM)

From the experimental test model was generated using a Leica TC1010 total station, a Kodak DCS460 camera, and IMAGINE OrthoBase Pro imaging software. Three low-cost digital cameras were calibrated using an external calibration method and the OrthoBase Calibration software. Photographs taken from the low-cost digital cameras generated digital elevation models that were compared to the reference DEM. The results of the study show that the low-cost digital cameras generated DEMs close to the true DEM. Proper lens calibration improved the accuracy of the results.

Tommaselli (2005) [9] performed to demonstrate the capability of taking 3 digital photographs and distance measurements from a mounted position of a flat element and obtaining the dimensions. This was done by finding the position of the camera relative to the flat element.

Jauregui (2006) [10] explained the study of a multi-station setup of a large grid of targets, scale bars, and camera stations were used to provide control points in 3D. The models used Photomodeler and AutoCAD. Errors between photogrammetric values and hand measurements had a maximum of 1.43%.

Close-range photogrammetry techniques have been shown to provide a simple and cost effective approach to historical building documentation Arias (2007) [11] submitted a paper explaining a case study of traditional agro-industrial building models taken from a multi-station setup of 2 plumb lines, 24 camera positions and 27 control points. The data were input into Photomodeler Pro 4.0 and obtained a root-mean-square error of 9mm for the model.

Shashi and Kamal (2007) [12] explained that the study 3D models of architectural structures is very important for analyses and also to reconstruct and document these structures. Visualization of these models allows the user to get the photo realistic impression of the structures than graphic based object models. 3D visualization has many applications in the areas of architecture, civil engineering, tourism, etc. Normally, field surveys are more accurate than photogrammetric measurements; nevertheless, they involve more personnel and consume a lot of time. Photogrammetry is a measurement technology that can be used for the extraction of 3D points from photographs. Their paper highlights the project using Photogrammetry for accurate 3D modeling and visualization of structures.

Sakir and Murat (2008) [13] showed that to determine the body measurements of a Holstein cow from its photographs with photo analysis, an environment for taking the photograph, a platform and 18 points with certain coordinates were prepared. Afterwards, the photos of a Holstein cow were taken on the platform with a Nikon D100 CCD camera from various directions. The photos were analyzed by PhotoModeler 5 software. The results of this image analysis were compared to real results that were previously measured. They found out that the real measurements and measurements obtained from photos are close to each other which show that this method can be safely used.

Sotoodeh and Gruen (2008) [14] reviews the whole workflow from data acquisition to the final geometrical surface and textural information. The results of the processes are presented and discussed and some conclusions regarding the exploitation of the two mentioned techniques are given. An antique 300-year old wooden globe, preserved in

the National Museum of Switzerland, had to be copied physically for delivery to another party. For this purpose a 3D computer model had to be generated. A structured light system and two digital frame cameras were employed, and the generated data sets were integrated to obtain both the geometry and the texture of the model.

Hullo and Fares (2009) [15] presented two kinds of models in this paper. The first application is the modeling of epigraphs from a single stereopair during prospection. Another application has been established on the site of Kilwa, where a building has been photographed and modeled. For this model, we got about 50 pictures. We inserted it on a Digital Elevation Model of the site obtained by tachometry in order to meet the needs of the architects and archaeologists and to make assumptions about the original condition of the site. The main advantage of this photogrammetric methodology is to get at the same time a point cloud (resolution depends on the size of the pixel on the object), and therefore a mesh, and oriented high resolution images. After processing, we can use the data exactly as a laser scanning point cloud, with really better raster information for textures.

1.3 Research Objective

The objectives of this research are to introduce photogrammetry as a 3D digitization technique which can be effective in documentation and digitization of the cultural heritage.

The aim of this work is the establishment of an efficient and accurate digital camera calibration method to be used in particular working conditions.

Two major aspects are studied in this research. Firstly, data acquisition and 3D model generation and secondly, and the second is using photogrammetric software package Photomodeler Scanner (version 6) as a measurement device to obtain 3D points with high accuracy.

1.4 Thesis Structure

This thesis consists of five chapters, described as following:

1. Chapter one gives a general view about the research deals with review of literature and
2. Chapter two represented fundamentals of analytical close range photogrammetry
3. Chapter three deals with data processing in analytical close range photogrammetry
4. Chapter four the photogrammetry consist with PhotoModeler software.
5. Chapter five deals with the experimental work and results analyses.
6. Chapter six Chapters five is devoted to gives several conclusions and recommendations for future works about the subject of thesis.

CHAPTER TWO

FUNDAMENTALS OF ANALYTICAL CLOSE RANGE PHOTOGRAMMETRY

2.1 Introduction

Analytical Photogrammetry can be considered as the mathematical transformation between an image point in one rectangular coordinate system (image space) and an object point in another rectangular coordinate system (object space). This basic mathematical concept is valid for all applications of analytical Photogrammetry (aerial, terrestrial and close range) using any sensing device to record directional information to object. Departures from the basic system take the form of mathematical models which describe the internal geometry of the sensor (camera) and the external geometry of object space. The two fundamental coordinate systems employed are the image coordinate system and the object space coordinate system [16].

The photogrammetrists have always tried to justify their efforts, the basis that they should be able to obtain more accurate results in less time than in the instrumental approaches, the basic material used in all these are the photographs, negatives or dispositive of various types. The basic inputs are the photo coordinates in a (x, y) (rectangular 2D) system. The output may be of various types, like X, Y, Z ground coordinates, orientation parameters, derived information on specific relations and conditions, etc. [17].

2.2 Photogrammetric Devices

Of all the different types of imaging systems used in the recording of data for photogrammetric measurements, the camera system is most frequently employed. When carried in an aircraft, it is referred to as an aerial camera; when fixed at a ground station, it can be called a terrestrial camera. The photogrammetrist divided the cameras used in Photogrammetry into two categories: metric and non-metric cameras [18].

2.2.1 Metric cameras

A metric camera is commonly associated with aerial cameras having an approximate focal length of 6 inches (152 mm). The photographic format size from these cameras is 9 by 9 inches. Frame cameras have fiducial marks positioned within the camera body. The fiducial marks are exposed onto the film emulsion when the photography is captured. The fiducial marks are subsequently measured to determine the interior orientation of the camera. Frame cameras are considered metric cameras since they have been calibrated in a laboratory [20].

2.2.2 Non-Metric Cameras

The photogrammetrist speaks of "non-metric camera", when the internal geometry of the camera is not stable and unknown, as is the case with any public used camera.

Although various types of metric cameras are available, there is a considerable use for non-metric cameras that are immediately available. The use of non-metric cameras, as opposed to metric cameras, for photogrammetric purposes has the following advantages and disadvantages:

The advantages are:

1. General availability.
2. Flexibility in focusing range.
3. Some are motor drive, allowing for quick succession of photographs.
4. Can be hand-held and there by oriented in any direction.
5. The price is considerably less than for metric cameras.

The disadvantages are:

1. The lenses are designed for high resolution at the expense of high distortion.
2. Instability of interior orientation.
3. Lack of fiducial marks.
4. Absence of level bubbles and orientation provisions precludes the determination of exterior orientation before exposure [19].

Figure (2-1), terrestrial metric camera

Figure (2-2) digital non-metric camera [34]

Figure (2-3) photogrammetric metric camera [34]

2.2.3 Camera Calibration

After a camera has been assembled by the manufacturer, it must be calibrated to determine the metrical characteristics needed for subsequent photogrammetric operations. These consist of:

1. The focal length of the camera lens.
2. The radial and tangential distortions of the lens.
3. The position of the principal point with respect to the fiducial marks.
4. The distances between the fiducial marks.
5. Flatness of the focal plane.

Basically, the purpose of camera calibration is to be able to reconstruct the precise geometry of the bundle of rays that entered the camera at the instant of exposure from the-dimensional measurement of points on the resulting photograph. This reconstruction is performed either graphically, instrumentally, or mathematically [18].

In general, camera calibration methods may be classified into one of three basic categories; (1) laboratory methods (2) field methods (3) self calibration method.

2.2.3.1 Laboratory Calibration methods

Laboratory methods are most frequently utilized and are normally performed by camera manufacturers [20].

2.2.3.2 Field Calibration methods

In the field procedures, the general approach consists of photographing an array of targets whose relative positions are accurately known. Elements of interior orientation are then determined by making precise measurements of the target images and comparing their actual imaged locations with positions they should have occupied had the camera produced a perfect perspective view [20].

2.2.3.3 Self-Calibration method

In this procedure the mathematical model (collinearity equations) is modified such that the observation equations include additional parameters to correct for systematic model or image coordinate errors. The additional parameters may be chosen according to the anticipated physical sources of

systematic errors (e.g. lens distortion, film deformation, etc). Another method may be to base the choice of additional parameters on geometrical considerations (e.g. to correct certain patterns of deformations) disregarding the actual sources of the error. Different types of polynomials have been proposed to compensate for various patterns of deformations [21].

2.3 Coordinate Systems

Conceptually, photogrammetry involves establishing the relationship between the camera or sensor used to capture the imagery, the imagery itself, and the ground. In order to understand and define this relationship, each of the three variables associated with the relationship must be defined with respect to a coordinate space and coordinate system [23].

2.3.1 Pixel Coordinate System

The file coordinates of a digital image are defined in a pixel coordinate system. A pixel coordinate system is usually a coordinate system with its origin in the upper-left corner of the image, the x-axis pointing to the right, the y-axis pointing downward, and the units in pixels, as shown by axes c and r in Figure (2-4). These file coordinates (c, r) can also be thought of as the pixel column and row number, respectively [23].

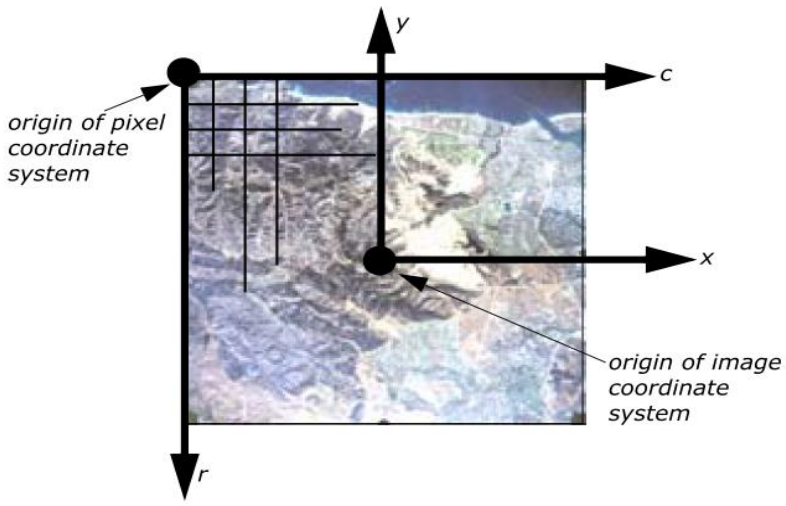

Figure (2-4): Pixel Coordinates vs. Image Coordinates [23].

2.3.2 Image coordinates system

An image coordinate system or an image plane coordinate system is usually defined as a two-dimensional (2D) coordinate system occurring on the image plane with its origin at the image center. The origin of the image coordinate system is also referred to as the principal point. On aerial photographs, the principal point is defined as the intersection of opposite fiducial marks as illustrated by axes x and y in Figure (2-4). Image coordinates are used to describe positions on the film plane. Image coordinate units are usually millimeters or microns [23].

2.3.3 Image Space Coordinate System

An image space coordinate system is identical to an image coordinate system, except that it adds a third axis (z) to indicate elevation. The origin of the image space coordinate system is defined at the perspective center S as shown in Figure (2-5). The perspective center is commonly the lens of the camera as it existed when the photograph was captured. Its x-axis and y-axis are parallel to the x-axis and y-axis in the

image plane coordinate system. The z-axis is the optical axis; therefore the z value of an image point in the image space coordinates system is usually equal to -f (the focal length of the camera). Image space coordinates are used to describe positions inside the camera and usually use units in millimeters or microns. This coordinate system referenced as image space coordinates (x, y, z) in this chapter [23].

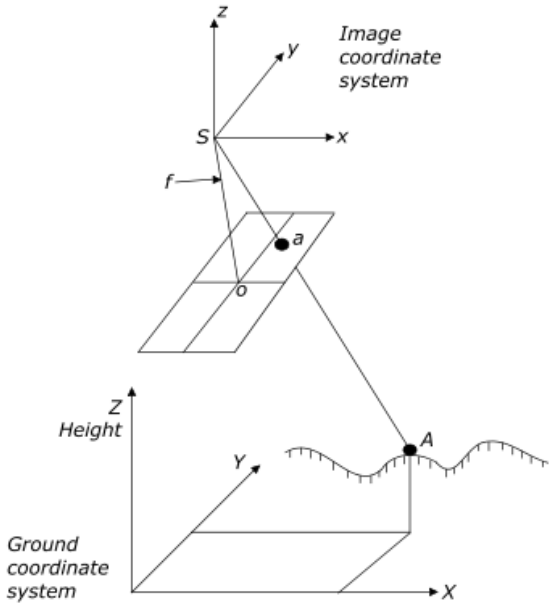

Figure (2-5) Image Space and Ground Space Coordinate System [23].

2.3.4 Ground coordinates system

A ground coordinate system is usually defined as a 3D coordinate system that utilizes a known geographic map projection. Ground coordinates (X, Y, Z) are usually expressed in feet or meters. The Z value is elevation above mean sea level for a given vertical datum. This coordinate system referenced as ground coordinates (X, Y, Z) in this chapter [23]. The geometric relationship between image and object is established by the exterior orientation. It defines the position and orientation of the image in object space. The six elements of exterior

orientation is the three object space coordinates X_L, Y_L, Z_L of the perspective centre (exposure station) and the three orientation angles φ,ω,κ of the image space coordinate axes with respect to the object space system. These angular elements are also referred to as X-tilt, Y-tilt and swing respectively to signify the axes around which the rotations occur, or as roll, pitch and yaw in terms of the attitude changes of the sensor platform [19].

2.4 Geometric Relationship between an Object and an Image

2.4.1 The interior orientation parameters (I.O.P)

The three fundamental elements of interior orientation are the two coordinates of the principal point x_0, y_0 in the fiducial system, and the principal distance c (figure 2-6). There are other factors that have an effect on interior orientation, which includes the radial and tangential lens distortion [19].

The radial lens distortion is expressed as:

$$dr = k_1r^3 + k_2r^5 + k_3r^7 \quad \text{…….. (2.1)}$$

or in *x* and *y* components:

$$dr_x = (k_1r^2 + k_2r^4 + k_3r^6)\,(x - x_o) \quad \text{……. (2.2)}$$

$$dr_y = (k_1r^2 + k_2r^4 + k_3r^6)\,(y - y_o) \quad \text{…….. (2.3)}$$

Where

k_1, k_2, k_3: are the coefficients of the polynomial.

r: is radial distance of the measured point from the principal point.

x_o, y_o: are the principal point coordinates.

x, y: are the measured image coordinates.

The decentring lens distortion model is given as:

$$dp_x = p_1(r^2 + 2(x - x_o)^2) + 2p_2(x - x_o)\,(y - y_o) \quad \text{… (2.4)}$$

$$dp_y = p_2(r^2 + 2(y - y_o)^2) + 2p_1(y - y_o)(y - y_o) \quad \ldots (2.5)$$

Where

dp_x, dp_y: are the decentring distortions in the x and y directions.

p_1, p_2: are the coefficients of the decentring model.

Accordingly the (I.O.P) = (x_0,y_0,c,k1,k2,k3,p1,p2)

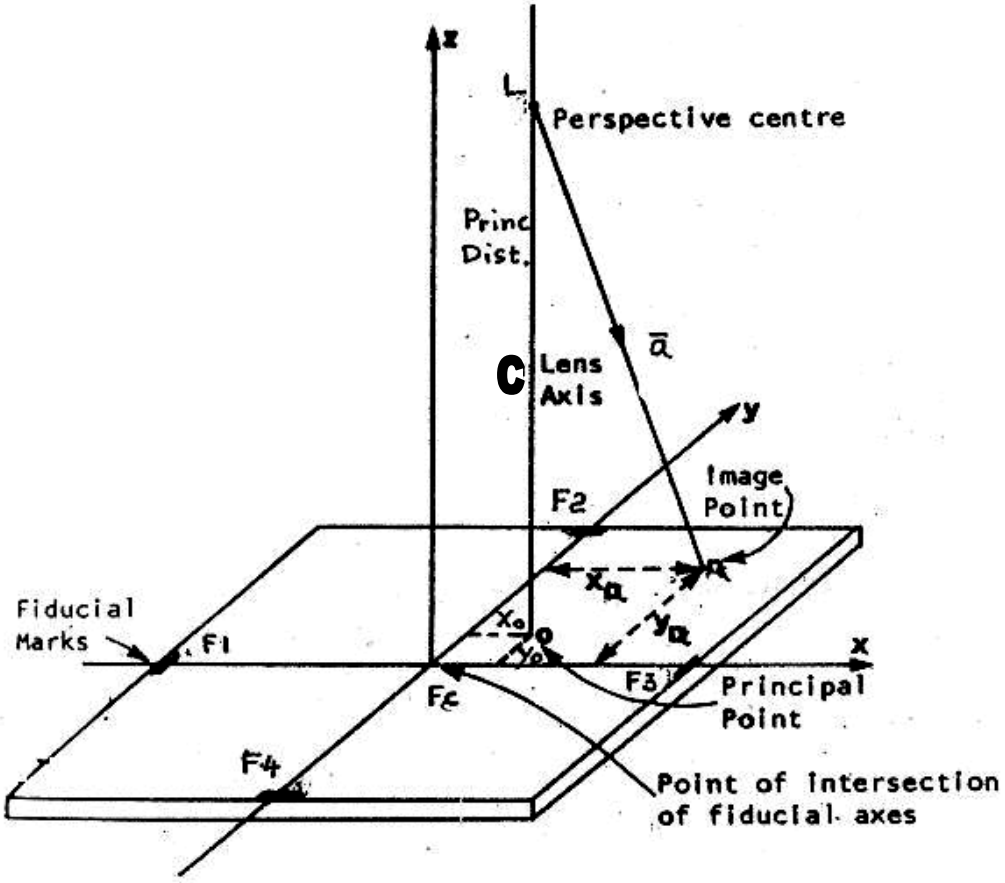

Figure (2-6) Interior Orientation [19]

2.4.1.1 Principle Distance

The image space coordinate system has its origin at the principal point, which is the foot of the perpendicular dropped from the perspective center onto the image plane. The x and y axes lie in the image plane and the positive z-axis is perpendicular to this plane. The three axes constitute a right-handed Cartesian coordinate system. The distance between the

perspective center and the principal point, or in other words, the length of the perpendicular dropped from the perspective central to the image plane, is called the principal distance or camera constant as shown in figure (2-7) [19].

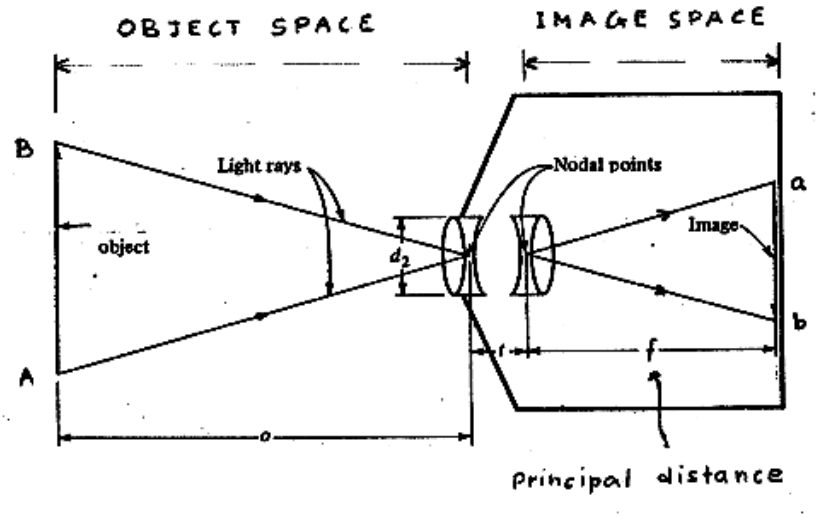

Figure (2-7) Principal Distance [19]

The principal distance is often referred to, erroneously, as focal length, although; the two quantities are not identical. Focal length is an optical quantity. It is the distance from the optical center of a lens measured along the optical axis to the point where rays coming from infinity intersect (focus or focal point). It is an inherent property of the lens assembly only and not of the camera assembly. It is determined by optical test procedures. The principal distance on the other hand is a geometric quantity pertaining to the entire camera assembly and is determined by camera calibration. To add to the confusion, in many literatures, both quantities are denoted as "f". Therefore, it is preferred to use the term camera constant denoted as "c". In fact the principal distance is more closely related to the optical quantity image distance, which appears in the lens equation, than to the focal length. As the camera is focused to various object distances, the image distance is

changing and so does, by definition, the principal distance, while the focal length remains constant. For cameras focused to infinity the three quantities are very nearly the same since the image plane is in the first optical condition requires that the lens equation to be satisfied in order to produce a sharp image on the easel plane. The rectifier has to be set so that

$$\frac{1}{i} + \frac{1}{p} = \frac{1}{F} \qquad \ldots\ldots \quad (2.6)$$

Where (i) is the image distance (the distance from the negative plane 'to the lens plane), (p) the projection distance (the distance from the easel plane to the lens plane) and (F) the focal length of the rectifier lens [19].

2.4.2 The Exterior Orientation parameters (E.O.P)

It defines the position and orientation of the image in object space. The six elements of exterior orientation are the three object space coordinates X_L, Y_L, Z_L of the perspective center (exposure station) and the three orientation angles (ω,φ,κ) of the image space coordinate axes with respect to the object space system (See Figure 2-8). These angular elements are also referred to as X-tilt, Y-tilt and Z-swing respectively to signify the axes around which the rotations occur, or as roll, pitch and yaw in terms of the attitude changes of the sensor platform. Accordingly the (E.O.P) = (X_L, Y_L, Z_L, ω, φ, κ) [19].

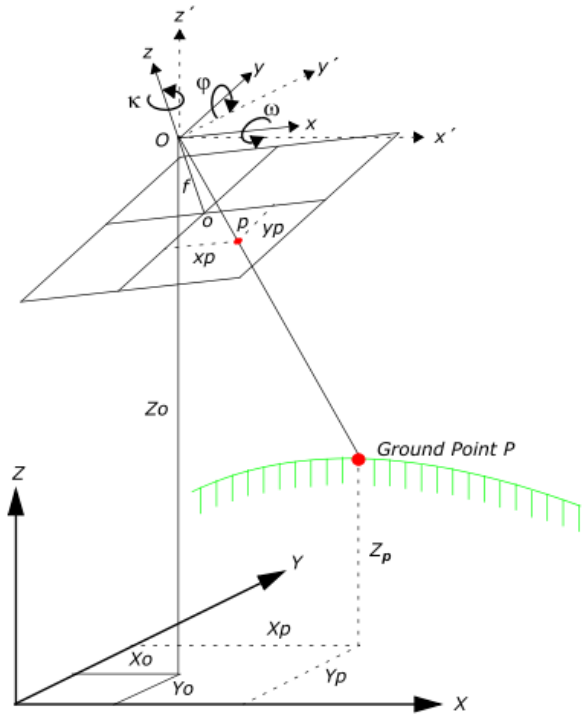

Figure (2-8) Exterior Orientation [lps]

2.5 Mathematical Modeling in Analytical photogrammetry

The collinearity condition specifies that the exposure station, ground point, and its corresponding image point location must all lie along a straight line, thereby being collinear.

2.5.1 Analytical Projective Relations in Arial photogrammetry

Imaging by central projection is based on the fundamental theorems that at the instant of projection, the perspective center L, the image point a, and the object point A, lie on a straight line. In other words the image vector, a and the object vectors A are collinear. See Figure (2-9). This so-called collinearity condition is valid for every ray in an imaging bundle and forms the basis of imaging with all types of sensors and for the reconstruction of objects from their images.

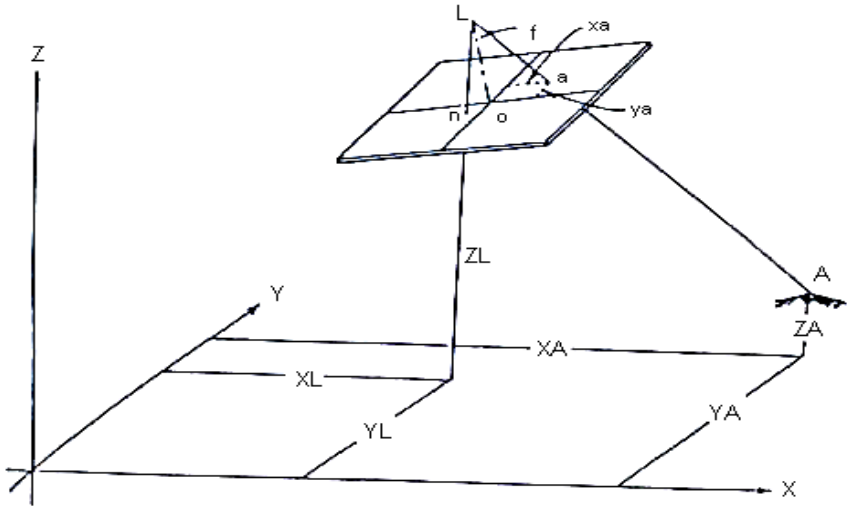

Figure (2-9), collinearity condition equations [١٩]

Two vectors are collinear if one is a scalar multiple of the other [١٩]. Whereby

$\bar{a}$=k $\bar{A}$

Where k is a scale factor.

The components of $\bar{a}$ in the image space coordinate system are

$$a = \begin{pmatrix} x_a - x_o \\ y_a - y_o \\ -c \end{pmatrix} \quad \text{…….. (2.7)}$$

And the components of $\bar{A}$ in the object space system are:

$$A = \begin{pmatrix} X_A - X_L \\ Y_A - Y_L \\ Z_A - Z_L \end{pmatrix} \quad \text{……. (2.8)}$$

The two vectors are now referred to a common coordinate system by transforming A from the object space system to the image space with the help of the orientation matrix M. Thus

$\bar{a}$=kM $\bar{A}$

Or

$$\begin{pmatrix} x_a - x_o \\ y_a - y_o \\ -c \end{pmatrix} = kM \begin{pmatrix} X_A - X_L \\ Y_A - Y_L \\ Z_A - Z_L \end{pmatrix} = k \begin{pmatrix} U \\ V \\ W \end{pmatrix} \quad \ldots\ldots\ldots (2.9)$$

By expanding M, performing the multiplication and dropping subscripts a and a results in the equation

$$x - x_o = k[m_{11}(X - X_L) + m_{12}(Y - Y_L) + m_{13}(Z - Z_L)] \quad \ldots\ldots. (2.10)$$

$$y - y_o = k[m_{21}(X - X_L) + m_{22}(Y - Y_L) + m_{23}(Z - Z_L)] \quad \ldots\ldots (2.11)$$

$$-c = k[m_{31}(X - X_L) + m_{32}(Y - Y_L) + m_{33}(Z - Z_L)] \quad \ldots\ldots.. (2.12)$$

The scalar k, which is different for each ray in a bundle, can be eliminated by dividing the first two equations with the third one. The final form of the equation is obtained as:

$$x - x_o = -c \frac{[m_{11}(X-X_L)+m_{12}(Y-Y_L)+m_{13}(Z-Z_L)]}{[m_{31}(X-X_L)+m_{32}(Y-Y_L)+m_{33}(Z-Z_L)]} = -c \frac{U}{W} \quad \ldots\ldots.. (2.13)$$

$$y - y_o = -c \frac{[m_{21}(X-X_L)+m_{22}(Y-Y_L)+m_{23}(Z-Z_L)]}{[m_{31}(X-X_L)+m_{32}(Y-Y_L)+m_{33}(Z-Z_L)]} = -c \frac{V}{W} \quad \ldots\ldots\ldots (2.14)$$

The two equations above are nonlinear to linearized using Taylor's theorem as described in appendix (A). After linearization and simplification we can obtain the Esq. (A-7) and (A-8), which is rewritten here as follows:

$$V_x = b_{11}d\omega + b_{12}d\phi + b_{13}d\kappa - b_{14}dX_L - b_{15}dY_L + b_{16}dZ_L + b_{14}dX + b_{15}dY - b_{16}dZ + J$$

$$V_y = b_{21}d\omega + b_{22}d\phi + b_{23}d\kappa - b_{24}dX_L - b_{25}dY_L + b_{26}dZ_L + b_{24}dX + b_{25}dY - b_{26}dZ + K$$

Where:

V_X and V_y	: Residual errors in measured x and y image coordinates.
$d\omega$, $d\phi$ and $d\kappa$	: Corrections to initial approximations for the orientation angles of the photo.
dX_L,dY_L,and dZ_L	: Corrections to initial approximations for the exposure station coordinates.
dX, dY, and dZ	: Corrections to initial value of the object space coordinates of the point.
$b's$, J and K	: Coefficients to be compute [appendix A].

2.5.2 Analytical Projective Relations in Close Range and Terrestrial Analytical photogrammetry

There is a simple difference between the terrestrial collinearity equations and the aerial collinearity equations.

In case of aerial photograph the image axes x, y and z are parallel to the X, Y and Z object space axes, respectively.

In case of terrestrial photograph image axis x is parallel to the object axis X, but image axes y and z are parallel to the object axes Z and Y respectively [20]. The terrestrial collinearity condition is illustrated in figure (2.10).

The form of collinearity equations in case of terrestrial photogrammetry is as follows:

$$x - xo = -c\left[\frac{m_{11}(X - X_o) + m_{12}(Z - Z_o) + m_{13}(Y_o - Y)}{m_{13}(X - X_o) + m_{32}(Z - Z_o) + m_{33}(Y_o - Y)}\right] \quad \text{..... (2.15)}$$

$$y - yo = -c\left[\frac{m_{21}(X - X_o) + m_{22}(Z - Z_o) + m_{23}(Y_o - Y)}{m_{31}(X - X_o) + m_{32}(Z - Z_o) + m_{33}(Y_o - Y)}\right] \quad \text{..... (2.16)}$$

Where:

x, y: the image point coordinates.

X, Y, Z: the object point coordinate.

X_o, Y_o, Z_o: the coordinates of the exposure station in the object space system.

c: the camera principle distance.

m's: the elements of rotation matrix.

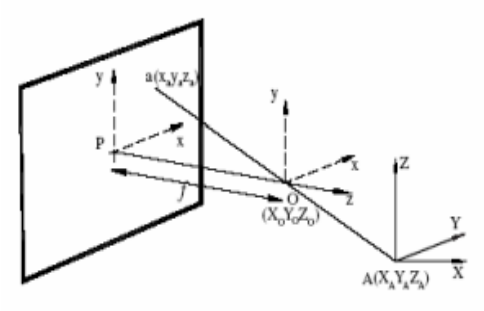

Figure (2.10): *Geometry of Terrestrial and Close Range Photogrammetry*

CHAPTER THREE

DATA PROCESSING IN ANALYTICAL CLOSE RANGE PHOTOGRAMMETRY

3.1 General Aspect

In general there are two approaches for data processing in analytical photogrammetry; first approach represent the sequential or simultaneous (bundle) solution, in this approach we are dealing with each photographs independently through the mathematical relation collinearity equation between each photo points its ground (space) location, a summary of the mathematical model for the sequential as well as simultaneous solution will be given in discussion next section. On the other hand, the second approach represent analytical relative orientation and absolute orientation, in this approach we are dealing with stereomodel constructed by relative orientation of the photos to a selected referenced photo and there after relate the constructed stereomodel to the natural (actual) ground model which is so-called absolute orientation, simply through the use of three dimensional conformal transformation. The mathematical modeling of this approach (relative and absolute orientation) will be discussion in details in section (3-3). In this research the second approach was used for data processing through the application of the Photomodeler Software.

3.2 Data processing by Sequential or simultaneous Solution

3.2.1 Sequential Solution

Sequential Solution consists of the following two computational steps:

3.2.1.1 Space Resection

Space resection by collinearity is a method of determining the six elements of exterior orientation (ω, ϕ, κ, X_L, Y_L, and Z_L) of a photograph. This method requires a minimum of three control points. It involves formulating the so-called collinearity equations for a number of control points whose X, Y, and Z ground coordinates are known and whose images appear in the tilted photo. The equations are then solved for the six unknown parameters of exterior orientation, which appear in them. The linearized forms of the space resection collinearity equations are [22]:

$$v_x = b_{11}d\omega + b_{12}d\phi + b_{13}d\chi - b_{14}dX_L - b_{15}dY_L - b_{16}dZ_{L+J} \quad \ldots. (3.1)$$

$$v_y = b_{21}d\omega + b_{22}d\phi + b_{23}d\chi - b_{24}dX_L - b_{25}dY_L - b_{26}dZ_L + K \quad \ldots. (3.2)$$

Where:

v_x & v_y Residual errors in measured χ&y image coordinates

$d\omega, d\phi, \& d\chi$ Corrections to initial approximations for the orientation angles of the photo

$dX_L, dY_L, \& dZ_L$ Corrections to initial approximations for the exposure station coordinates

$b's$ Coefficients, which are described in appendix (A)

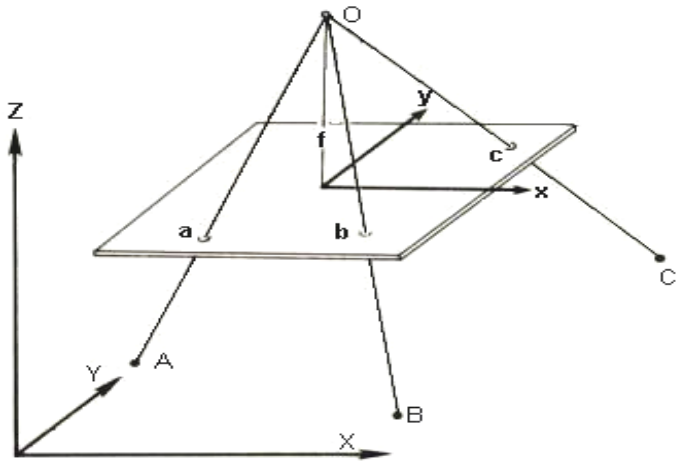

Figure (3-1) Space Resection [22].

With two equations possible for each control points, a total of six equations are obtained from three control points. This system of equations is solved simultaneously for the six unknown corrections, and these corrections are then added to initial values to obtain revised values. The solution is made again using the revised values as initial estimates, and new correction are calculated. This procedure is iterated until the magnitudes of the corrections become negligible. If more than three control points are available, then more than six equations can be formulated and their solution can be obtained by the method of least squares. The mathematical model for the single photo space resection is:

$$_{2n}A^{1}\ _{6}X^{1} = {}_{2n}L^{1} + {}_{2n}V^{1} \qquad \ldots (3.3)$$

Where

$$A = \begin{bmatrix} b_{11_i} & b_{12_i} & b_{13_i} & -b_{14_i} & -b_{15_i} & -b_{16_i} \\ b_{21_i} & b_{22_i} & b_{23_i} & -b_{24_i} & -b_{25_i} & -b_{26_i} \end{bmatrix} \quad X = \begin{bmatrix} \partial\omega \\ \partial\emptyset \\ \partial k \\ \partial X \\ \partial Y \\ \partial Z \end{bmatrix}$$

$$L = \begin{bmatrix} J_i \\ K_i \end{bmatrix} \qquad V = \begin{bmatrix} v_{x_i} \\ v_{y_i} \end{bmatrix}$$

Where

n= number of points

i = 1: n

3.2.1.2 Space Intersection

The collinearity equations may also be used to determine X, Y, and Z ground coordinates of new points whose images appear in the overlap area of a stereo pair of tilted photos. The procedure is known as space

Intersection. Space intersection requires that the six parameters of exterior orientation for the two overlapping titled photos be known (which have been computed in the previous step). The linearized forms of the space intersection equations for point P are [22]:

$$v_{xp} = b_{14}dX_p + b_{15}dY_p + b_{16}dZ_p + J \quad \ldots\ldots (3.4)$$

$$v_{yp} = b_{24}dX_p + b_{25}dY_p + b_{26}dZ_p + K \quad \ldots\ldots (3.5)$$

Where:

v_{x_p} & v_{yp} Residual errors in measured *x&y* image coordinates of point *p*

dX_p, dY_p, dZ_p Corrections to initial values of the object space coordinates of the point *P*

$b's$ Coefficients, which are described in appendix (A)

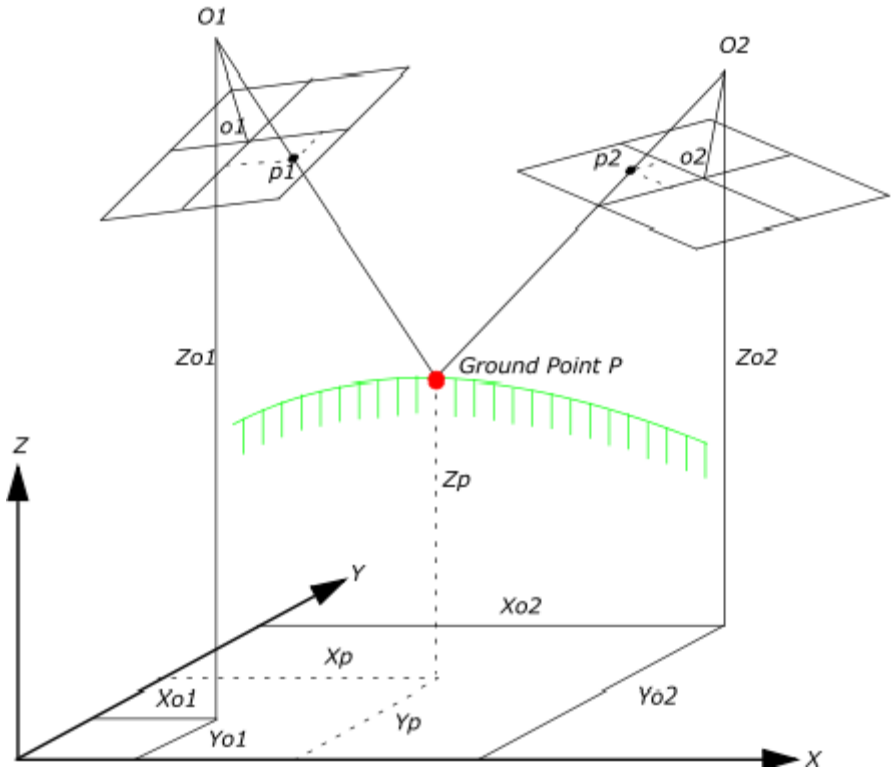

Figure (3-2), Space Intersection [23].

Figure (3-2) shows the space intersection with stereo pair of the tilted photographs. Two equations can be written for point P at each of the two overlapping photos; hence four equations result, and the value of $dX_P, dY_P,$ and dZ_P can be computed in a least squares solution. The corrections are applied to the initial approximations to obtain revised values for Xp, Yp, and Zp. The solution is then repeated until the magnitudes of the corrections become negligible [22]. The mathematical model for the two photos intersection is:

$$v_1 + A^s{}_1 X + F_1 = 0 \qquad \text{The first photo} \qquad \dots (3.6)$$

$$v_2 + A^s{}_2 X + F_2 = 0 \qquad \text{The second photo} \qquad \dots (3.7)$$

$$v + A_i^s X^s + F = 0 \qquad \dots (3.8)$$

Where i= 1: n

n= number of points

$$A_i^s = \begin{bmatrix} B_1^s \\ B_2^s \end{bmatrix} \qquad B_1^s = \begin{bmatrix} (b_{14_i})_1 & (b_{15_i})_1 & (b_{16_i})_1 \\ (b_{24_i})_1 & (b_{25_i})_1 & (b_{26_i})_1 \end{bmatrix}$$

$$B_2^s = \begin{bmatrix} (b_{14_i})_2 & (b_{15_i})_2 & (b_{16_i})_2 \\ (b_{24_i})_2 & (b_{25_i})_2 & (b_{26_i})_2 \end{bmatrix}$$

$$v_i = \begin{bmatrix} v_{x_i} \\ v_{y_i} \end{bmatrix} \quad X = \begin{bmatrix} dX_i \\ dY_i \\ dZ_i \end{bmatrix} \qquad F_i = \begin{bmatrix} J_i \\ K_i \end{bmatrix}$$

3.2.2 Simultaneous (Bundle) Solution

The process is named bundle adjustment because of the many light rays that pass through each lens position constituting a bundle of rays. The bundles from all photos are adjusted simultaneously so that corresponding

light rays intersect at positions of the target points [23]. The mathematical model of Bundle Adjustment is the collinearity equations, e. g. a point in object space, its corresponding point in the image plane and the projective center of the camera lie on a straight line [24].

Since the terrestrial collinearity equations are not linear, they are linearized by applying the first order terms of Taylor's series at a set of initial approximations. After linearization the observation equations can be expressed in the following matrix form [16]:

$$V_{ij+}B_{ij}^{e}\Delta_{i}^{e}+B_{ij}^{s}\Delta_{j}^{s}=f_{ij} \qquad \ldots (3.9)$$

Where

$$B_{i}^{e}=\begin{bmatrix} b_{11ij} & b_{12ij} & b_{13ij} & -b_{14ij} & -b_{15ij} & b_{16ij} \\ b_{21ij} & b_{22ij} & b_{23ij} & -b_{24ij} & -b_{25ij} & b_{26ij} \end{bmatrix}$$

$$B_{i}^{s}=\begin{bmatrix} b_{14ij} & b_{15ij} & -b_{16ij} \\ b_{24ij} & b_{25ij} & -b_{26ij} \end{bmatrix}$$

$$\Delta_{i}^{e}=\begin{bmatrix} d\omega i \\ d\varphi i \\ d\kappa i \\ dX_{oi} \\ dZ_{oi} \\ dY_{oi} \end{bmatrix};\ \Delta_{i}^{s}=\begin{bmatrix} dX_{oi} \\ dZ_{oi} \\ dY_{oi} \end{bmatrix},\ f_{ij}=\begin{bmatrix} J_{ij} \\ K_{ij} \end{bmatrix}$$

The subscripts *(i)* and *(j)* in the above terms are used for photo number and point number, respectively. The matrix B_{ij}^{e} contains the partial derivatives of the collinearity equations with respect to the exterior orientation parameters of photo *i*, evaluated at the initial approximations.The matrix B_{ij}^{s} contains the partial derivatives of the collinearity equations with respect to the object space coordinates of point *j*, evaluated at the initial approximations. Matrix Δ_{i}^{e} contains corrections for the initial approximation of the exterior orientation parameters for photo *i*, and matrix

Δ_j^s contains corrections for the initial approximation of the object space coordinates for point *j*.

3.3 Mathematical model of digital camera calibration

This calibration is based on the method of space resection . It is based on collinearity equation, take image point coordinates as observations, and get to internal and external orientation elements of the camera, distortion factor and other additional parameters. Take account of the correct item, the collinearity equations are:

$$(x - x_0) + \partial x = -c\frac{m_{11}(X-X_L)+m_{12}(Y-Y_L)+m_{13}(Z-Z_L)}{m_{31}(X-X_L)+m_{32}(Y-Y_L)+m_{33}(Z-Z_L)} \quad \ldots\ldots\ldots\ldots (3.10)$$

$$(y - y_0) + \partial y = -c\frac{m_{21}(X-X_L)+m_{22}(Y-Y_L)+m_{23}(Z-Z_L)}{m_{31}(X-X_L)+m_{32}(Y-Y_L)+m_{33}(Z-Z_L)} \quad \ldots\ldots (3.11)$$

Where

$\partial x, \partial y =$ an additional parameter represent the lens distortion (radial and tangential)

$$\delta x = x'(k_o + k_1 r^2 + k_2 r^4 + \ldots) + p_1(r^2 + 2x'^2) + 2p_2 x' y'$$

$$\delta y = y'(k_o + k_1 r^2 + k_2 r^4 + \ldots) + 2p_2 x' y' + p_2(r^2 + 2y'^2)$$

The mathematical model of collinearity equations with addition parameters are:

$$AV + B^e\Delta^e + B^i\Delta^i + B^s\Delta^s + E = 0 \ldots\ldots\ldots\ldots\ldots (3.12)$$

Where A, B^e, B^i, B^s are the coefficient matrices in which

$$A_{2n*2n}=\begin{bmatrix}\partial F(x)/\partial(x,y)\\ \partial F(y)/\partial(x,y)\end{bmatrix} \qquad B^{e}{}_{2n*6m}=\begin{bmatrix}\partial F(x)/\partial(e.o)\\ \partial F(y)/\partial(e.o)\end{bmatrix}$$

$$B^{i}{}_{2n*ap}=\begin{bmatrix}\partial F(x)/\partial(AP)\\ \partial F(y)/\partial(AP)\end{bmatrix} \qquad B^{s}{}_{2n*3n}=\begin{bmatrix}\partial F(x)/\partial(X,Y,Z)\\ \partial F(y)/\partial(X,Y,Z)\end{bmatrix}$$

n=no. of points

m=no. of photo

aP=no. of additional parameters

Due to the form of the central projection equations, matrix A is equal to the identity matrix.

The vectors of alteration Δ, of residuals V, and of discrepancies E are expressed explicitly as [21]:

$$\Delta^{e}{}_{6m*1}=\begin{bmatrix}d\omega\\ d\varphi\\ d\kappa\\ dX_{L}\\ dY_{L}\\ dZ_{L}\end{bmatrix} \quad ; \qquad \Delta^{i}{}_{ap*1}=\begin{bmatrix}d_{AP}\end{bmatrix} \quad ; \qquad \Delta^{s}{}_{3n*1}=\begin{bmatrix}dX\\ dY\\ dZ\end{bmatrix}$$

3.4 Data Processing by Relative and Absolute Orientation

In photogrammetry for most applications are taken so that adjacent photos overlap by more than 60 percent. Two adjacent that overlap in this manner form a stereopair, and object points that appear in the overlap area constitute a stereomodel. The mathematical calculation of three-dimensional ground coordinates of points in the stereomodel by analytical

photogrammetric techniques forms an analytical stereomodel. The process of forming an analytical stereomodel involves three primary steps: interior orientation (described in previous chapter), relative orientation, and absolute orientation. After these three steps are achieved, points in the analytical stereomodel will have object coordinates in the ground coordinates system [22].

3.4.1 Analytical Relative Orientation

Analytical relative orientation is the process of determining the relative angular attitude and positional displacement between the photographs that existed when the photos were taken. This involves defining certain elements of exterior orientation and calculating the remaining ones. The resulting exterior orientation parameters will not be the actual values that existed when the photographs were exposed; however, they will be adjusted in a "relative sense" between the photos. In analytical relative orientation, it is common practice to fix the exterior orientation elements ω, ϕ, κ, X_L, and Y_L of the left photo of the stereopair to zero values. Also for convenience, Z_L of the left photo (Z_{L1}) is set equal to f, and X_L of the right photo (X_{L2}) is set equal to the photo base b.

This leaves five elements of the right photo that must be determined [22]. Figure (3-3) illustrates a stereomodel formed by analytical relative orientation.

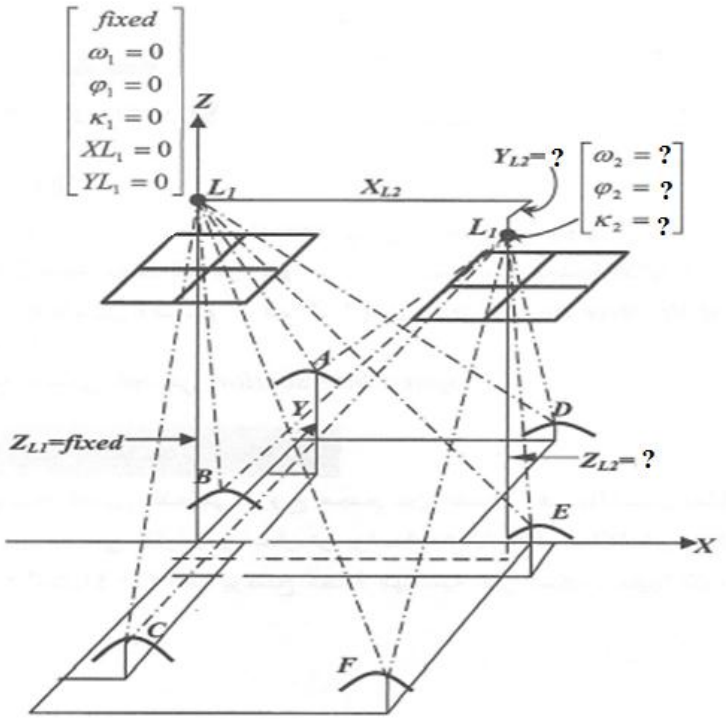

Figure (3-3) Analytical relative orientation of stereopair [22].

Although the coplanarity condition equation can be used for analytical relative orientation, the collinearity condition is more commonly applied. In applying collinearity equation, each object point in the stereomodel contributes four equations: a pair of equations for x and y photo coordinates of its image in the left photo, and a pair of equations for x and y photo coordinates of its image in the right photo. In addition to five unknown orientation elements, each object point adds three more unknowns which are their X, Y, and Z coordinates in the stereomodel. Thus, each point used in relative orientation results in a net gain of one equation for the overall solution, and therefore at least 5 object points are required for a solution. If 6 or more points are available, an improved solution is possible through least squares method. In figure (3-3) six points were used in analytical relative orientation. In matrix form, the system of 24 equations involving 23 unknown when n number of point, m number of photo could be expressed as follows:

$$_{2nm}A^{3n+5}\ _{3n+5}X^{1} = {}_{2nm}L^{1} + {}_{2nm}V^{1} \quad \ldots (3.13)$$

Where

$$A = \begin{bmatrix} {}_2O^5 & {}_2B^s_{1a} & {}_2O^3 & {}_2O^3 & {}_2O^3 & {}_2O^3 & {}_2O^3 \\ {}_2O^5 & {}_2O^3 & {}_2B^s_{1b} & {}_2O^3 & {}_2O^3 & {}_2O^3 & {}_2O^3 \\ {}_2O^5 & {}_2O^3 & {}_2O^3 & {}_2B^s_{1c} & {}_2O^3 & {}_2O^3 & {}_2O^3 \\ {}_2O^5 & {}_2O^3 & {}_2O^3 & {}_2O^3 & {}_2B^s_{1d} & {}_2O^3 & {}_2O^3 \\ {}_2O^5 & {}_2O^3 & {}_2O^3 & {}_2O^3 & {}_2O^3 & {}_2B^s_{1e} & {}_2O^3 \\ {}_2O^5 & {}_2O^3 & {}_2O^3 & {}_2O^3 & {}_2O^3 & {}_2O^3 & {}_2B^s_{1f} \\ {}_2B^e_{2a} & {}_2B^s_{2a} & {}_2O^3 & {}_2O^3 & {}_2O^3 & {}_2O^3 & {}_2O^3 \\ {}_2B^e_{2b} & {}_2O^3 & {}_2B^s_{2b} & {}_2O^3 & {}_2O^3 & {}_2O^3 & {}_2O^3 \\ {}_2B^e_{2c} & {}_2O^3 & {}_2O^3 & {}_2B^s_{2c} & {}_2O^3 & {}_2O^3 & {}_2O^3 \\ {}_2B^e_{2d} & {}_2O^3 & {}_2O^3 & {}_2O^3 & {}_2B^s_{2d} & {}_2O^3 & {}_2O^3 \\ {}_2B^e_{2e} & {}_2O^3 & {}_2O^3 & {}_2O^3 & {}_2O^3 & {}_2B^s_{2e} & {}_2O^3 \\ {}_2B^e_{2f} & {}_2O^3 & {}_2O^3 & {}_2O^3 & {}_2O^3 & {}_2O^3 & {}_2B^s_{2f} \end{bmatrix}$$

$$X = \begin{bmatrix} \Delta^e_2 \\ \Delta^s_a \\ \Delta^s_b \\ \Delta^s_c \\ \Delta^s_d \\ \Delta^s_e \\ \Delta^s_f \end{bmatrix} \quad V = \begin{bmatrix} \gamma_{1a} \\ \gamma_{1b} \\ \gamma_{1c} \\ \gamma_{1d} \\ \gamma_{1e} \\ \gamma_{1f} \\ \gamma_{2a} \\ \gamma_{2b} \\ \gamma_{2c} \\ \gamma_{2d} \\ \gamma_{2e} \\ \gamma_{2f} \end{bmatrix} \quad L = \begin{bmatrix} \varepsilon_{1a} \\ \varepsilon_{1b} \\ \varepsilon_{1c} \\ \varepsilon_{1d} \\ \varepsilon_{1e} \\ \varepsilon_{1f} \\ \varepsilon_{2a} \\ \varepsilon_{2b} \\ \varepsilon_{2c} \\ \varepsilon_{2d} \\ \varepsilon_{2e} \\ \varepsilon_{2f} \end{bmatrix}$$

The terms of these matrices are from Esq. (A-7) and (A-8) and the method of calculating each is explained in appendix (A). The subscripts a, b, c, d, e, and *f* correspond to the point names in figure (3-3). Subscript 1 refers to the left photo; and subscript 2 refers to the right photo.

$$_2O^5 = \begin{bmatrix} 0 & 0 & 0 & 0 & 0 \\ 0 & 0 & 0 & 0 & 0 \end{bmatrix} \qquad _2O^3 = \begin{bmatrix} 0 & 0 & 0 \\ 0 & 0 & 0 \end{bmatrix}$$

$$B^{e}_{2p}=\begin{bmatrix}(b_{p11})_2 & (b_{p12})_2 & (b_{p13})_2 & (-b_{p15})_2 & (-b_{p16})_2\\ (b_{p21})_2 & (b_{p22})_2 & (b_{p23})_2 & (-b_{p25})_2 & (-b_{p25})_2\end{bmatrix}$$

$$B^{s}_{2ip}=\begin{bmatrix}(b_{p14})_i & (b_{p15})_i & (b_{p16})_i\\ (b_{p24})_i & (b_{p25})_i & (b_{p26})_i\end{bmatrix}$$

$$\Delta^{e}_{2}=\begin{bmatrix}d\omega_2\\ d\emptyset_2\\ dk_2\\ dY_{L2}\\ dZ_{L2}\end{bmatrix} \qquad \Delta^{s}_{p}=\begin{bmatrix}dX_p\\ dY_p\\ dZ_p\end{bmatrix} \qquad \varepsilon_{ip}=\begin{bmatrix}(J_p)_i\\ (K_p)_i\end{bmatrix} \qquad \gamma_{ip}=\begin{bmatrix}(\gamma_{xp})_i\\ (\gamma_{yp})_i\end{bmatrix}$$

Where

In the above submatrices, (p) is the point designation, and (i) is the photo designation. The prefixed subscript and postfixed subscript designate the number of rows and columns, the (b's) coefficients to be computed in [appendix A].

When the observation equations are partitioned in the above manner, the least squares solution $(A^TA)X=(A^TL)$ takes the following form.

$$\begin{bmatrix}N_2^e & \bar{N}_a & \bar{N}_b & \bar{N}_c & \bar{N}_d & \bar{N}_e & \bar{N}_f\\ \bar{N}_a^T & N_a^s & {}_30^3 & {}_30^3 & {}_30^3 & {}_30^3 & {}_30^3\\ \bar{N}_b^T & {}_30^3 & N_b^s & {}_30^3 & {}_30^3 & {}_30^3 & {}_30^3\\ \bar{N}_c^T & {}_30^3 & {}_30^3 & N_c^s & {}_30^3 & {}_30^3 & {}_30^3\\ \bar{N}_d^T & {}_30^3 & {}_30^3 & {}_30^3 & N_d^s & {}_30^3 & {}_30^3\\ \bar{N}_e^T & {}_30^3 & {}_30^3 & {}_30^3 & {}_30^3 & N_e^s & {}_30^3\\ \bar{N}_f^T & {}_30^3 & {}_30^3 & {}_30^3 & {}_30^3 & {}_30^3 & N_f^s\end{bmatrix}\begin{bmatrix}\Delta_2^e\\ \Delta_A^s\\ \Delta_B^s\\ \Delta_C^s\\ \Delta_D^s\\ \Delta_E^s\\ \Delta_F^s\end{bmatrix}=\begin{bmatrix}k_2^e\\ k_A^s\\ k_B^s\\ k_C^s\\ k_D^s\\ k_E^s\\ k_F^s\end{bmatrix}$$

Where

$$N_2^e = \sum_{p=a}^{f} B_{2p}^{e^t} B_{2p}^e \quad \text{(5×5 submatrixe)} \quad \dots (3.14)$$

$$\bar{N}_p = B_{2p}^{e^t} B_{2p}^s \quad \text{(5×3 submatrixe)} \quad \dots (3.15)$$

$$N_p^s = \left(B_{1p}^{s^t} B_{1p}^s\right) + \left(B_{2p}^{s^t} B_{2p}^s\right) \quad (3 \times 3\ submatrix) \quad \dots (3.16)$$

$$k_2^e = \sum_{p=a}^{f} B_{2p}^{e^t} \varepsilon_{2p} \quad (5 \times 1\ submatrix) \quad \dots (3.17)$$

$$k_p^s = \left(B_{1p}^{s^t} \varepsilon_{1p}\right) + \left(B_{2p}^{s^t} \varepsilon_{2p}\right) \quad (3 \times 1\ submatrix) \quad \dots (3.18)$$

$$_3 0^3 = \begin{bmatrix} 0 & 0 & 0 \\ 0 & 0 & 0 \\ 0 & 0 & 0 \end{bmatrix}$$

3.4.2 Analytical Absolute Orientation

For a small stereomodel such as that computed from one stereopair, analytical absolute orientation can be performed using a three-dimensional conformal coordinate transformation. This requires a minimum of two horizontal and three vertical control points, but additional control points provide redundancy, which enables a least squares solution. In the process of performing absolute orientation, stereomodel coordinates of control points are related to their three-dimensional coordinates in a ground based system. It is important for the ground system to be a true cartesian coordinate system, such as local vertical, since the three-dimensional conformal coordinate transformation is based on straight, orthogonal axes [22].

3.4.2.1 Three-dimensional conformal coordinate transformation equation

A three-dimensional conformal coordinate transformation involves converting from one three-dimensional system to another. In the transformation, true shape is retained. This type of coordinate transformation is essential in analytical or computational photogrammetry for two basic problems:

(1) To transform arbitrary stereomodel coordinates to a ground or object space system and (absolute orientation).

(2) To form continuous three-dimensional "strip model" from independent stereomodels.

Three-dimensional conformal coordinate transformation equations are developed here in general. In figure (3-4) it is required to transform coordinates of points from an *xyz* system to an *XYZ* system [22].

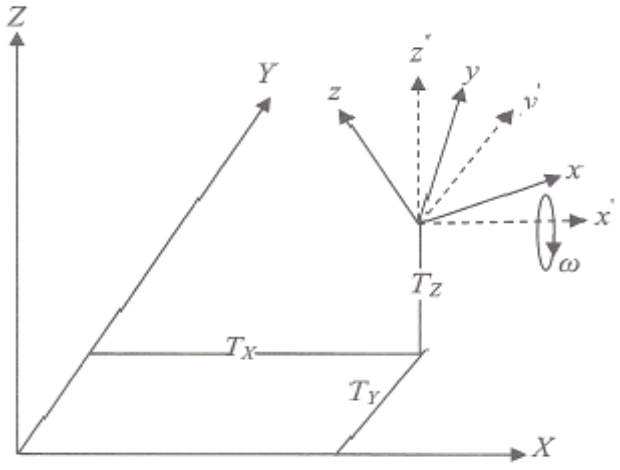

Figure (3-4) ***XYZ*** and ***xyz*** right-handed three-dimensional coordinate systems [22].

As illustrated in the figure, the two coordinate systems are at different scales, they are not parallel, and their origins do not coincide. The necessary transformation equations can be expressed in terms of seven parameters; the three rotation angles omega (ω), phi (ϕ), and (κ); a scale

factor (s); and three translation parameters T_X, T_Y, and T_Z. Before proceeding with the development of the transformation equations, it is important to define sign conventions. All coordinates shell defined as in right-handed. Rotation angles (ω, ϕ, κ) are positive if they are counterclockwise, for example, positive ω rotation about x' axis is shown in figure (3-4).

The mathematical derivation of the three dimensional conformal transformation is the exactly similar to that of the collinearity equation gives in the appendix (A). Which can by surmised in the following two basic steps:

(1) Rotation

As apparent in figure (3-4) with three steps to convert from xyz system to apply to x'y'z' system: The mathematical derivative of these three steps is discussed in appendix (B). After rotation angles (ω, ϕ, κ) about axes. Substituting m's for coefficients of *x'*, *y'*, and *z'* gives

$$x = m_{11}x' + m_{12}y' + m_{13}z'$$

$$y = m_{21}x' + m_{22}y' + m_{23}z'$$

$$z = m_{31}x' + m_{32}y' + m_{33}z' \qquad (3\text{-}19)$$

Equation (3-19) may be expressed matrix form as

$$X = MX' \qquad (3\text{-}20)$$

Where

$$X = \begin{bmatrix} x \\ y \\ z \end{bmatrix} \qquad m = \begin{bmatrix} m_{11} & m_{12} & m_{13} \\ m_{21} & m_{22} & m_{23} \\ m_{31} & m_{32} & m_{33} \end{bmatrix} \quad and \; X' = \begin{bmatrix} x' \\ y' \\ z' \end{bmatrix}$$

The rotation matrix is orthogonal matrix, which has the property that its inverse is equal to its transpose, or

$$M^{-1} = M^T \tag{3-21}$$

Eq. (3-20) may be rewritten, expressing x' y' z' coordinate in terms of x y z coordinates as follows:

$$X' = M^T X \tag{3-22}$$

In expanded form this equation is:

$$x' = m_{11}x + m_{21}y + m_{31}z$$

$$y' = m_{12}x + m_{22}y + m_{32}z$$

$$z' = m_{13}x + m_{23}y + m_{33}z \tag{3-23}$$

(2) Scaling and Translation

To arrive at the final three-dimensional coordinate transformation equations, equations that yield coordinates in the *XYZ* system of figure (3-4), it is necessary to multiply each of Eqs. (3-23) by a scale factor (*s*) and to add the translation factors T_X, $T_{Y,}$ and $T_{Z.}$ to convert (*x'*, *y'*, *z'*) system coordinate to (*X*, *Y*, *Z*) system coordinate as shown in figure (3-4). This step makes the lengths of any lines equal in both coordinate

systems, and it translates from the origin of $x'y'z'$ to the origin of the *XYZ* system. Performing this step yields

$$X = sx' + T_X = s(m_{11}x + m_{21}y + m_{31}z) + T_X$$

$$Y = sy' + T_Y = s(m_{12}x + m_{22}y + m_{32}z) + T_Y$$
$$Z = sx' + T_Z = s(m_{13}x + m_{23}y + m_{33}z) + T_Z \quad (3\text{-}24)$$

In matrix form, Eqs. (3-24) are

$$\bar{X} = sM^T X + T \quad (3\text{-}25)$$

In Eq. (3-25), matrices *M* and *X* are as previously defined, *s* is the scale factor, and

$$\bar{X} = \begin{bmatrix} X \\ Y \\ Z \end{bmatrix} \qquad and \qquad T = \begin{bmatrix} T_X \\ T_Y \\ T_Z \end{bmatrix}$$

In eqs. (3-24) they are seven unknowns parameters, three rotation angles ω, ϕ, and κ its represented in rotation matrix m's, three unknown translations T_X, T_Y, and T_Z, and *s* scale factor for each points (P). These non linear equations (3-24) are linearized in appendix (B). Once the transformation parameters have been computed, they can be applied to the remaining stereomodel points, including the X_L, Y_L, and Z_L coordinates of the left and right photographs. This gives the coordinate of all stereomodel points in the ground system. Figure (3-5) illustrates analytical absolute orientation [22].

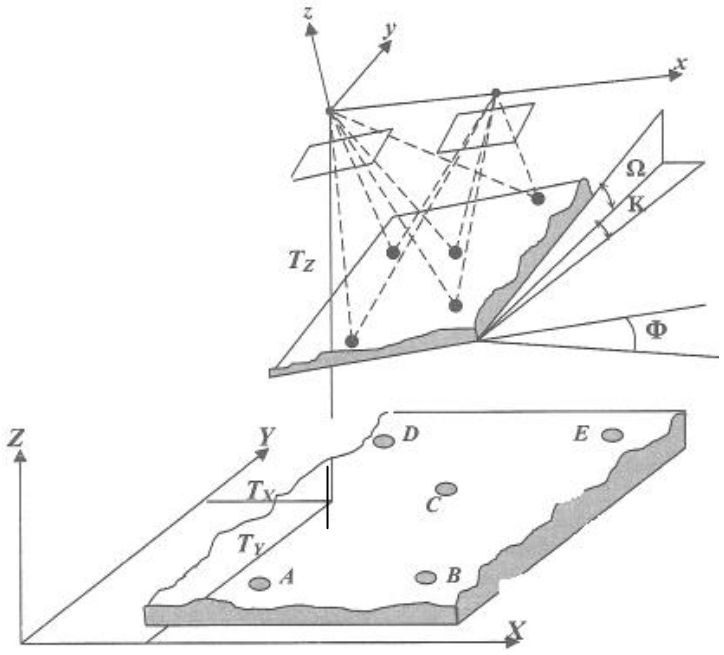

Figure (3-5) Analytical absolute orientation

The mathematical model of three-dimensional conformal transformation in analytical absolute processing.

$$\begin{bmatrix} X \\ Y \\ Z \end{bmatrix} = s \times M(\Omega, \Phi, K) \times \begin{bmatrix} x \\ y \\ z \end{bmatrix} + \begin{bmatrix} T_X \\ T_Y \\ T_Z \end{bmatrix} \quad \text{….. (3.26)}$$

Where: X, Y, Z Ground coordinates system

x, y, z Model coordinates system

$M(\Omega, \Phi, K)$ Rotation matrix

T_X, T_Y, T_Z Translation distance

s Scale factor

CHAPTER FOUR

PHOTOGRAMMETRY CONSISTENT WITH PHOTOMODEL SOFTWARE

4.1 General

The images can be saved in a format to be used with PhotoModeler, including JPEG, TIFF, BMP and PNG. To make a 3D model, photographs generated from traditional 35 mm film prints, digital cameras, as well as video images are used also. The EOS system that recommends at least two photos are taken to capture all the important aspects of the object, and that the areas of the images cover overlap each other. The points are then correlated from one 'references' photo with corresponding points on the other photos. Close-ups and wide shots can be combined in a project, and new details can be added at any time.

4.2 CLOSE-RANGE PHOTOGRAMMETRY METHOD

The term 'close-range photogrammetry' is used to describe the technique when the extent of the object to be measured is less than about 100 meters and cameras are positioned close to it [29]. In the past, close-range applications have been Distinguishable from topographic applications by size, appearance and shape of the objects and by the size of the images. The differences of the objects will remain for the future, but the size of the image data will get closer [30].

The result of close range photogrammetry must generally be made available very quickly after acquisition of, the images so that they can be used for further processing related to the measured object and its function. Derived coordinates might be used for comparing the measured object with

its designed size and shape in a test of conformance. They are sometimes processed further using computer graphics, for example to produce a three dimensional CAD (computer aided design) model of the object and in a few cases drawn and dimensional plans, elevations or sections may be required. The development of analytical photogrammetric techniques has enabled rapid growth in the applications of close-range photogrammetry. The ability to model the camera geometry mathematically, instead of relying on analog restitution allows the use of a wide variety of non-metric cameras. Through the use of analytical self-calibration techniques, accuracy has increased to the point where Close-range photogrammetry has become a standard technique for precision (Manufacture and service) industrial inspection.

Its primary applications are industrial, manufacturing, and facilities management; it therefore supports the import and export of data in standard CAD formats, so that the photogrammetrically produced measurements and models can be easily used for design or analysis. An example of such system is PhotoModeler, a product of EOS system [31]. PhotoModeler accepts photos from both un-calibrated and calibrated cameras. The system defines object in the scene by combinations of geometric primitives, such as cylinders or planes, and operator specifies points or edges to be used in the solution. The models produced can be exported in standard CAD or graphics formats.

4.3 PhotoModeler Scanner Software

PhotoModeler is a Windows software package for measuring and modeling real world objects and scenes through the use of photographs. PhotoModeler is a world leader in its class and it is based on the science of photogrammetry, which means measuring from photographs. PhotoModeler brings the powerful capabilities of photogrammetry in a

simple, easy-to-use Windows environment. It includes the exciting capability of scanning textured surfaces to create a dense cloud of points. PhotoModeler extracts measurements and 3D models from photographs by using a camera as an input device, and enables capturing accurate details in a short time. PhotoModeler is used in a number of application areas where measurement and modeling of the real-world is required. These are accident reconstruction, forensics, film and game production, architectural modeling, engineering and scientific applications and archaeology. The specific version of PhotoModeler used in this study was version 6 [25].

4.4 Establishing of 3D Modeling

The first step towards the establishment of a photo-based 3D modeling approach in support of construction simulating visualization. Our field trials lead to generalization of the basic workflow of the modeling method, which consists of two phases, namely: on-site photographing and in-lab post processing of photos (Figure 4.1).

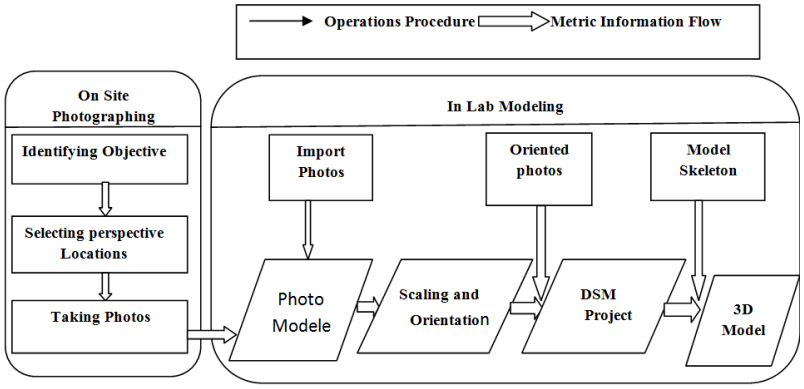

Figure (4.1): Basic workflow of photo-based modeling.

The phase of on-site photo taking is mainly concerned with acquiring adequate site photos, and these photos will provide input to later in-lab modeling. The on-site photographing phase is composed of three steps:

(1) identifying the object, (2) selecting perspective locations, and (3) taking photos. In the phase of in-lab modeling, as shown in Figure (4.1), the site photos are exported from the digital camera into the personal workstation with PhotoModeler software in order to sketch out the model skeleton in 3D. The model skeleton depicts the basic geometry outline of the desired object but may not be as complete as desired, since data as of some edges or vertices of a complex object could be missing in those site pictures. The resulting skeleton model can then be rendered into realistic 3D object scenes to use in site situation visualization or operations of simulation animation. Note rendering can be interpreted as the automatic process of converting 3D skeleton models (wireframes, dots, texture surfaces) into 3D object images with photorealistic effects on a computer.

4.4.1 Take Photographs of the Object or Scene

When positioning camera stations, one rule for implementing photogrammetry is that the closer the angle between the light rays (up to right angle), the smaller possible error will occur. In Figure (4.2) and (4.3), Station (1) has the same position and the same angle error, however, that placing Station (2) at an acute angle to Station (1) magnifies the small error, and thus the resulting position of the 3D point turns out much farther (Figure 4.3): in comparison with the result as shown in Figure (4.2)[25].

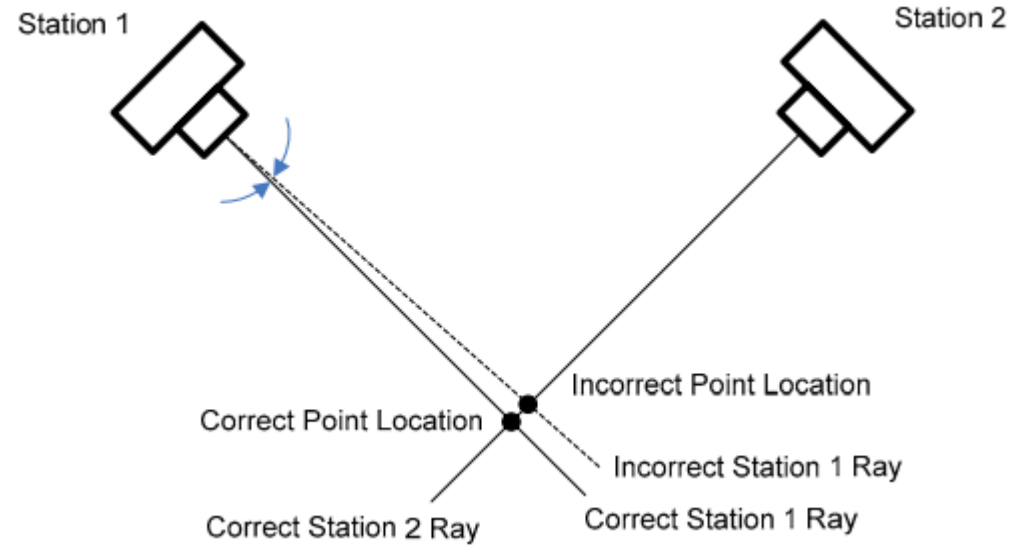

Figure (4.2): Point location error with good camera positions.

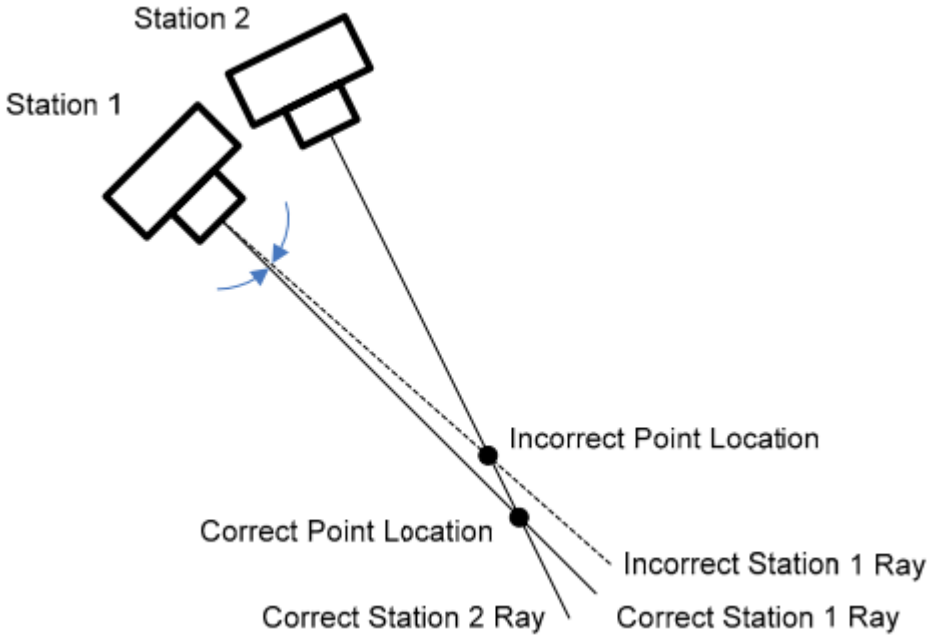

Figure (4.3): Point location error with bad camera positions.

Theoretically, one point being covered in two photos is sufficient for fixing the point in 3D coordinates. But in practice, imprecision in point marking may cause another form of error. Point marking is the interaction process for identifying points explicitly on the photos to inform the modeling algorithm where the points' positions are. To alleviate this error, the desired point should be preferably covered in three or more photographs at the expense of redundancy. As such, if the point was

positioned incorrectly on one of the photos, the other two could still compensate for the marking error.

To photograph a convex face of an object, normally three camera station positions would suffice. Figure (4.4) depicts the camera positioning layout. The camera stations are not at right angles to one another. Nonetheless, they are in proper positions to provide triple coverage of target points instead of double coverage. To photograph an alcove in an object usually requires more camera stations in comparison with photographing a convex face. Figure (4.5) shows the camera position layout for photographing an alcove object. In order to cover points A and B on three photographs respectively, extra station positions of C and D are recommended. The station C is inserted to ensure coverage for point B, while the station D targets at point A.

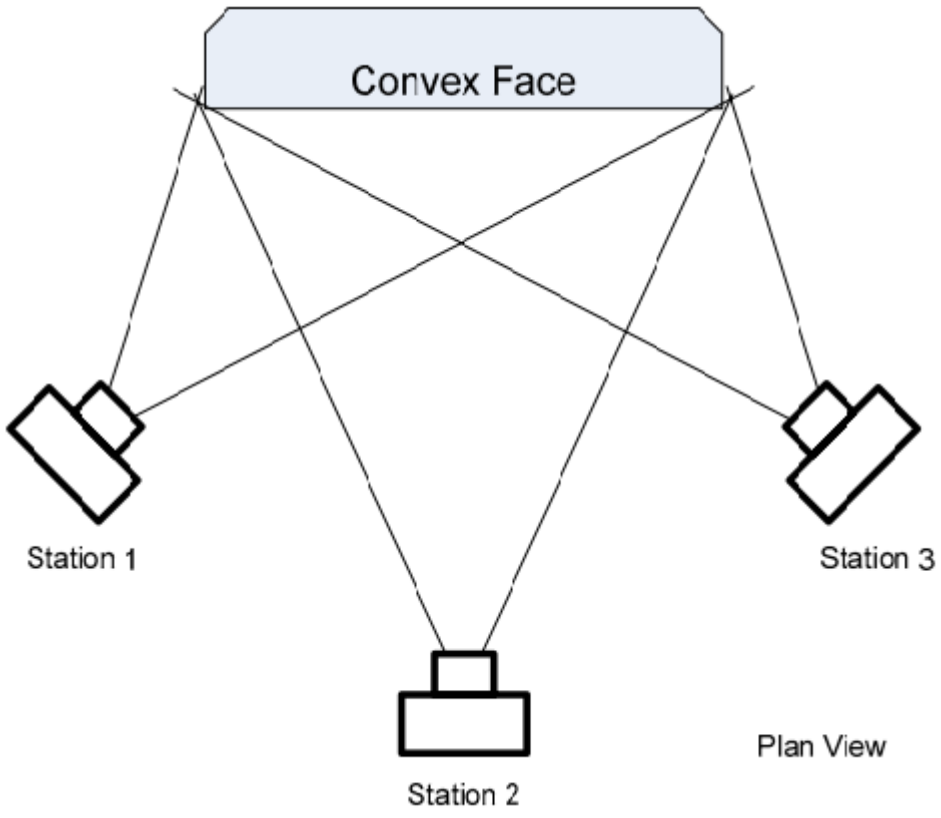

Figure (4.4): Camera station positions for a convex face.

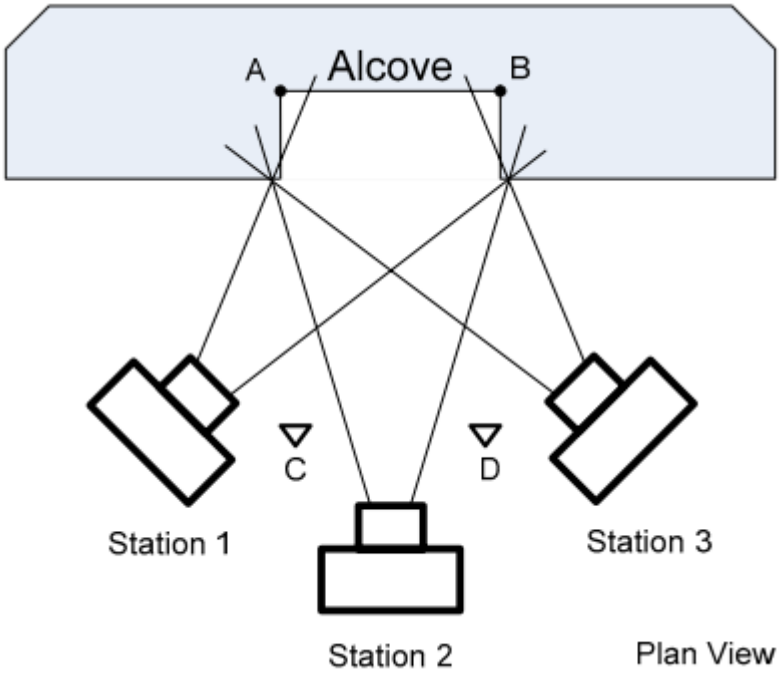

Figure (4.5): Camera station positions for an alcove.

4.4.2 PROCESS OF ESTABLISHING 3D MODEL FROM IMAGES

Following sub-sections discuss the process for developing the 3D Model from digital images by using PhotoModeler software on the case study project.

1. Select Data Analysis Software and Import the Images

With rapidly increasing capabilities of digital cameras and personal computers in recent years, some photogrammetry software's are made available. These products can analyze images from any source. Photomodeler, one of the consumer software products has been used successfully throughout this research. First, the images are transferred from the cameras to the computer by using USB flash drive. Before pictures can be transferred (copied) to computer, the supplied software must be installed. Then the Photomodeler software is started, and the images are

selected and imported into the program for analysis. Next, the user associates each image with its specific, previously calibrated camera.

2. Object preparation and scene arrangement

Before taking photos, the first step preparation of an object it is accomplished by deploying special markers on object in purposeful manner. Finding proper strategy of marker deployment is an important matter, it helps to find an optimum workflow between amount of work in item preparation, time of calculation and detailed result in point cloud.

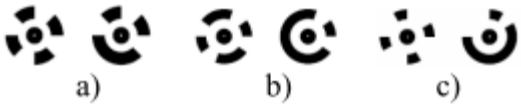

Figure (4.6): Coded targets, a) 8 bit, b) 10 bit, c) 12 bit.

The second stage of the analysis is scene arrangement – placing object between special coded targets. Using these symbols provides the possibility of automatic mutual photograph oriented during the later computing. Every coded target has unique shape, its unique digital representation, recognized by software tool, see figure (4.6). Sample model, placed on an arranged scene, ready for photographing is shown on figure (4.7).

Figure (4. 7): Artificial object with coded targets.

3. Mark the Target Locations in Each Image

Data analysis begins by marking the locations of the targets in the images. The xy coordinates of the centroid of each elliptical target projected while dots in this case, must be marked as accurately as possible in each image.

Targets are high contrast circles placed in a scene or on an object to provide an accurate sub-pixel point marking. Coded targets are circular targets with some additional bits that can be automatically recognized by PhotoModeler during the marking process see fig (4.8).

Figure (4.8): One of the coded targets.

Coded targets have different size depending on coverage of each photo in real world space and the camera parameters. Minimum target radius computed by using two formulas.

The first formula is the coverage formula and is appropriate when most of the targets are at similar distance from the camera. This formula does not require as much knowledge of the camera.

Minimum target radius = 5 * w / pw …… (4.1)

Where 'w' is the width of coverage of each image in real world space and 'pw' is the number of pixels in the width of the image.

The second formula is the "distance formula" and is appropriate when you know the approximate distance from the farthest coded target to

a camera position. This formula does require more knowledge of the camera parameters.

Minimum target radius = (5 * fw * D) / (f * pw) …… (4.2)

Where 'fw' is the format width of the camera, 'D' is the distance between the farthest target and a camera position, 'f' is the camera focal length, and 'pw' is the number of pixels in the width of the photo [25].

4. Identify Points in the Photos Referring to the Same Physical Point

The second step of the data analysis is to match the marked points in one photo with their corresponding points in the other photos. This process is called referencing the points. When a point is initially marked on an photo, it is assigned a unique identification number. When a marked point on one image is referenced to a marked point on another image, the software reassigns the same identification number to both points indicating they are the same physical location on the structure. In the beginning of the data analysis, the user must perform this referencing operation automatically or manually until a certain minimum number of points (at least six) are referenced on all photos, at time the user processes the data. When these calculations are completed, the user returns to the referencing phase. At this point, automatic helper tools are available to speed up the process. These tools appear as a result of the initial processing of the data, which yields the spatial location and orientation angles of the cameras. In figure (4.9) the viewer shows small camera icons at their locations and orientations relative to targets with calculated 3D coordinates, displayed as small dots. Now the images are said to be oriented.

5. Scaling and Orientation

After imported photos are taken with coded target to the Photomodeler, code target can be used to (Translate/Scale/Rotate) project. This type of coordinate system transformation is defined based on coded targets. There are three components that define the conformal transformation were defined by coded targets. For example code target number (1) in the grid of coded target is used to define the translation that has arbitrary value for the x, y, and z equal (0, 0, 0). Often the translation point is the origin (0, 0, 0) but it could be any coordinate value. The known distance between two coded targets used to define the scale in the model so that they can be determining absolute measurements in study model. Finally use the coded targets to define the axes of the coordinate system of the model as in the example, figure (4.9).

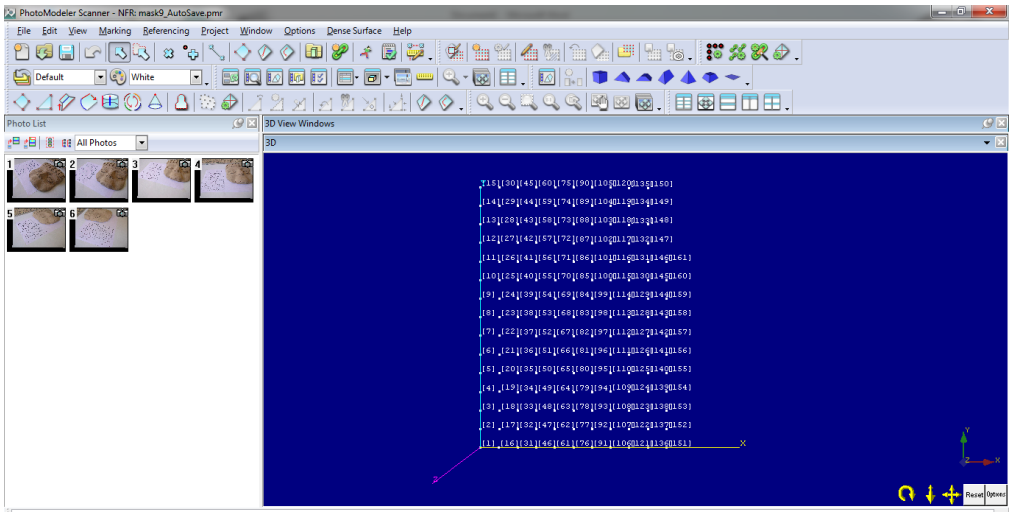

Figure (4.9): Using code targets to define Translate/Scale/Rotate**.**

Code target ID1 defines the Translate, and the distance between two ID'S (1, 15) defines the scale, the two ID'S in x-direction used to define X-axis and the two ID'S in the y-direction used to define Y-axis. The first axis that was defined becomes the 'dominant' axis. The two active axes should

be close to right angles. When the coordinate system is computed, PhotoModeler calculates the exact secondary axis at 90 degrees to the dominant axis based on the plane defined by the two axes.

Note: A Cartesian coordinate system in which the location of the third axis may be inferred from the location of the two other axes by using the right hand rule. This rule states that, if you form the first three fingers of your right hand into three perpendicular vectors, and point your thumb in the direction of the X axis, and your index finger in the direction of the Y axis, your middle finger will point in the direction of the Z axis.

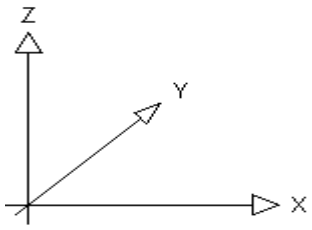

Figure (4.10): According to Right Hand rule.

4.4.3 Identify Points in the Images Refers to the Same Physical Point

The second step of the data analysis is to match the marked points in one image with their corresponding points in the other images. This process is called referencing the points. When a point is initially marked on an image, it is assigned a unique identification number. When a marked point on one image is referenced to a marked point on another image, the software reassigns the same identification number to both points indicating they are the same physical location on the structure. In the beginning of the data analysis, the user must perform this referencing operation manually until a certain minimum number of points (at least six) are referenced on all photos, at time the user processes the data. When

these calculations are completed, the user returns to the referencing phase. At this point, automatic helper tools are available to speed up the process. These tools appear as a result of the initial processing of the data, which yields the spatial location and orientation angles of the cameras. Now the images are said to be oriented. In a typical Photomodeler project without control points especially points with a known coordinates, the camera locations and orientations calculated above are relative quantities with respect to the camera. At this point, it is a good idea to verify that the software positioned the cameras properly, which can be checked easily in the graphical 3D viewer available in Photomodeler. The viewer shows small camera icons at their locations and orientations relative to targets with calculated 3D coordinates, displayed as small dots. Controls are available to rotate or resize the 3D graphic for better viewing as shown in Figure (4.11).

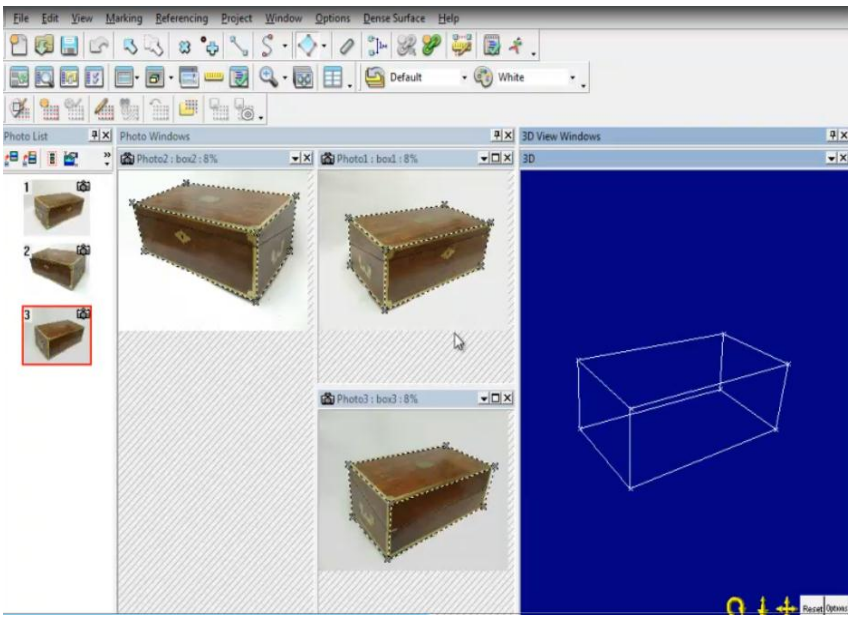

Figure (4.11): Marking on reference points and 3D viewer.

4.4.4 Idealize Module

The Idealized module will take an existing project and use the calibrated camera parameters to produce an idealized camera and images. That will re-map (pixel by pixel) any specified images and removing any lens distortion, non-centered principal point and any non-square pixels. It will then adjust the existing marks to match the undistorted image and then assign an idealized camera to the project. The resulting images and camera positions should then be suitable to be used in rendering packages that do not handle 'real world' cameras. An example of before and after Idealize:

Figure (4.12): Camera distortions removed by idealization.

This module provides the capability to convert the camera in the project from real form to ideal form. An ideal camera has no lens distortion, square pixels, and a centered principal point. The images in the project are resampled and the photographic marks are shifted to match the new idealized images.

After geometric correction, the photographs need to be related with the reference points to show the same objects on two or more

photographs on the software. When a sufficient number of points have been added, the software alerts the user that orientation may be possible.

A successful orientation produces a table of all images with base/height ratios and angulations for each image pair, information that allows the 3D viewer to show the interrelationship of scenes and reference points.

In the beginning of the laboratory works, iron objects and gypsum carvings coated in various colors was chosen to create a three dimensional model for them, and after finishing the requirements for the result, a three dimensional model was not exactly completed as there was a missing parts of the form caused by reflectional in such bodies. After that, an unpainted clay objects were used to conduct requirements mentioned above to produce three-dimensional model of clay objects and they were successfully obtained without any missing parts, because clay substance has the ability to absorb rays, it helps to represent all parts of the body in the digital image in good way.

CHAPTER FIVE

3D MODEL ESTABLISHMENT AND RESULTS ANALYSIS

5.1 Introduction

In this chapter, discussion of three cases of study before each of these cases calibration of the camera will be done after that photo will be taken to the object; first case takes five photos of the artificial object face-shape made of clay. These photos were imported to Photomodeler and referenced and oriented automatically after orientation of these photos. Photomodeler created stereomodel of the object, second case takes three photos to the small solid model in this case selected minimum five or more points with code target and without code target to reference manually to orient the photos. After orientation each point has three coordinate values (x, y, z) and the distance between points in this case were compared between PhotoModeler and Vernier device as a measurement tool. Finally takes two photos (out door) for building and processing them manually by Photomodeler to extract the accuracy of represented 3D points from the façade of this building.

5.2 Data processing with Photomodeler Software

The data processing with Photomodeler can be summarized as follow as:

1. Camera calibration
2. Relative orientation
3. Absolute orientation

The relative and absolute orientations are discussed in section (3-3) in chapter three because of the fact that Photomodeler represents an update development in close range photogrammetry. The calibration process by Photomodeler software will be discussed in details in section (4-4).

5.3 Description of Digital Camera

The two primary types of digital cameras were used in this research are Nikon (COOLPIX AW100 with resolution16 megapixels), its zoom (5-25) mm, and SANYO (E1075, resolution 10 megapixels), with zoom (5.7-17.1) mm. The shapes of these cameras are shown in figure (4.1) and (4.2) respectively, and the main characteristics of these cameras are illustrated as follows in two tables, (5.1) and (5.2) respectively.

Figure (5.1): Nikon Coolpix AW100 [32]

Figure (5.2): Sanyo (E1075) [33]

Table (5.1): Camera's Main Characteristics (Nikon) [32]

Type	Compact digital camera	
Effective Pixels	Approx. 16 mega pixels	
Image Sensor Size	1/2.3-in.type CMOS :Approx. 16.79 million pixels, (6.4286x4.8214) mm.	
Pixel Size	0.00139 mm; In appendix (C) you find a table with technical data of several CCD chips [26].	
Lens Mount	5x optical zoom. Nikkor lens	
Focal Length	(5-25)mm (angle of view equivalent to that of 28-140 mm)	
Recording pixels	(1) Large:	Approx. 16 mega pixels (4608 x 3456)
	(2) Medium:	Approx. 8.00 mega pixels (3264 x 2448)
	(3) Small:	Approx. 3 mega pixels (2048 x 1536)
	(4) RAW:	Approx. 16 mega pixels (4608 x 3456)
Focusing Modes	Focus range (from view) ,focus-area selection	
Focusing range	Approx. 50cm. (1ft-8in.) to ∞ (W); approx. 1m. to∞ (T)	
Shutter Speeds	1/1500sec. to 1secs.	
Depth-of-field preview	Enabled with depth-of-field preview button	
Image type	JPEG	

Table (5.2): Camera's Main Characteristics (SANYO) [33]

Type	Digital Camera	
Effective Pixels	Approx. 10 mega pixels	
Image Sensor Size	(6.4125x4.8094) mm	
Pixel Size	0.00175mm; In appendix (C) you find a table with technical data of several CCD chips.	
Lens Mount	3x optical zoom lens	
Recording pixels	(1) Large:	Approx. 10.00 mega pixels (3664 x 2748)
	(2) Medium:	Approx. 5.00 mega pixels (2048 x 1536)
	(3) Small:	Approx. 2.00 mega pixels (1600 x 1200)
	(4) RAW:	Approx. 10.00 mega pixels (3664x 2748)
Focusing Modes	Multi zone –center- selected area	
Shutter Speeds	1/2000sec. to 2secs.	
Depth-of-field preview	99% by LCD	
Image type	JPEG	

5.5 Camera Calibration

5.5.1 General

The first step in all projects with Photomodeler is calibrating the camera. Camera parameters commonly discovered through calibration procedures include the computed principal distance or focal length (c) of the lens, parameters (x_p, y_p), which denote the coordinates of the center of projection of the image (principal point), and lens distortion coefficients (k_1, k_2, k_3, p_1, p_2) where the terms k_i represent coefficients of radial lens distortion and p_i terms represent coefficients of decentring distortion caused by a lack of centering of lens elements [28]. For calibrating the camera, an accurate determination of the interior orientation parameters is needed. For more accurate results, the calibration images should be taken under conditions that are similar to the field samples.

A lab calibration based on a flat pattern to carry out the calibration Photomodeler Scanner software was conducted. The lab calibration process was completely automatic using a calibration grid. The focal length was fixed at narrowest and widest angle and the network includes a total of twelve images with ± 90º roll angles.

After the software processing, the camera calibration parameter values were obtained. The results and the accuracy of this calibration method, as well as the overall RMSs obtained from the calibration for both cameras are in micron.

5.5.3 Digital Camera Calibration

5.5.3.1 **Overview**

For the most accurate results, the camera must be field calibrated. To field calibrate, simply photograph a special grid (see Figure 5.3)

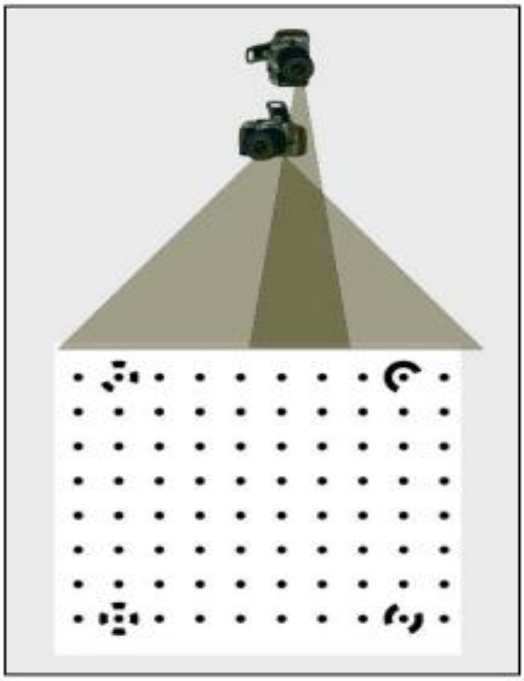

Figure(5.3): Calibration Grid Positions.

The grid can be found in the PhotoModeler Pro 6 folder (typically under program file in the c drive) and should be printed close to the size of the project. PhotoModeler has a special calibration project built-in. A calibration project requires that about 6 and 12 photos of the grid should be taken. For best results, a minimum of two photos should be taken per side, one in a landscape position and the other in a portrait position (See Figure 5.4 and Figure 5.5) respectively.

Figure (5.4): Landscape position.

Figure (5.5): Portrait Position.

GOOD vs. BAD

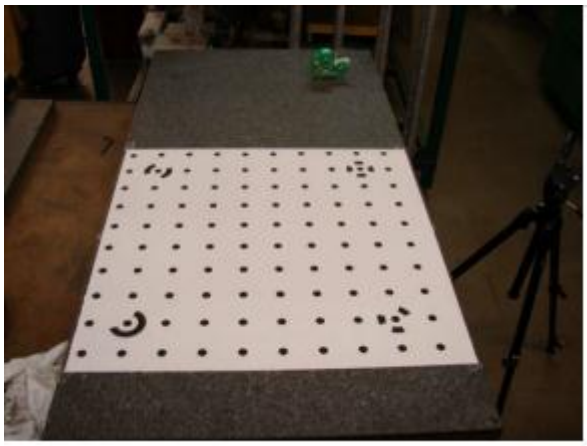

Figure (5.6): Bad Exposure.

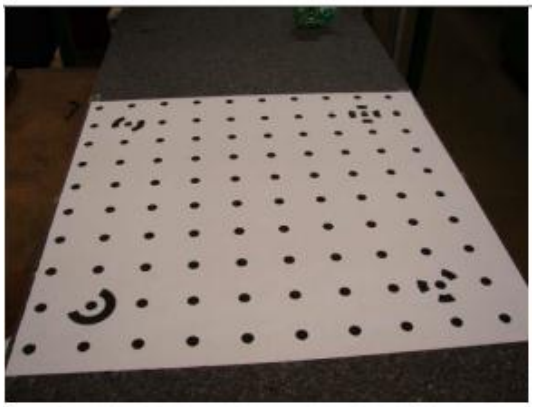

Figure (5.7): Good Exposure.

For the best results in both calibration and measurement photographs, take a step closer to the object. For example, the good photograph in Figure (5.7) with the calibration grid and the bad photograph in Figure (5.6) [25]. PhotoModeler software to establish the mathematical model of the digital camera, and locating points also calibrating the mathematic model. The image with standard calibration points printed on a piece of paper of a size (21 × 29.7) cm, then place the paper on the flat floor, the camera is fixed on a tripod, taking three photos from each of the four directions.

5.5.3.2 Calibration and results

Twelve images from different locations and different angles for each time are taken. In this study, each zoom is calibrated for five times. The results are illustrated in the following four tables in (5.3), (5.4), (5.5), and (5.6) respectively.

To ensure the calibration accuracy of the results, the obtained images should at least be full of 80% of the frame [27].

The calibration images should be taken under similar conditions to the lap samples for most accurate results. When using the PhotoModeler software for calculation, 12 images arranged at regular orientation.

Table (5.3): Calibration results of main parameters for camera Nikon (CoolpixAW100), with fixed focal length (5mm).

	Calibration(1)	**Calibration(2)**	**Calibration(3)**	**Calibration(4)**	**Calibration(5)**
c(mm)	5.2667±6.5E-4	5.2368±2 E-3	5.2637±8.8E-4	5.2652±5.2E-4	5.2646±5.9E-4
x_P(mm)	3.2665±5E-4	3.2655±1E-3	3.2726±7.7E-4	3.2697±4.5E-4	3.2693±5.5E-4
y_p(mm)	2.4295±6.4E-4	2.4137±2E-3	2.4278±8.5E-4	2.4262±5.1E-4	2.4282±6.5E-4
K1	-2.78E-4±1.9E-5	-7.29E-4±3.6E-5	-1.75E-4±2.9E-5	-1.88E-4±1.9E-5	-2.6E-4±2.3E-5
K2	-2.34E-6±1.2E-6	2.45E-5±2.6E-6	-5.824E-6±1.9E-6	-7.oo7E-6±1.2E-6	-2.929E-6±1.8E-6
K3	0	0	0	0	0
P1	-6.61E-4±6.7E-6	-6.549E-4±1.6E-5	-7.422E-5±1E-5	-6.967E-4±6.2E-6	-7.034E-4±7.3E-6
P2	1.869E-4±8.1E-6	-7.039E-5±2.2E-5	1.35E-4±1.1E-5	8.775E-5±6.7E-6	1.553E-4±8.4E-6
Image coverage (%)	90	88	82	84	88
Overall RMS (pixels)	0.3562	0.5497	0.4756	0.2869	0.3387
Δc(mm)	0.2667	0.2368	0.2637	0.2652	0.2646

Table (5.4): Calibration results of main parameters for camera, Nikon (CoolpixAW100) with fixed focal length (25mm).

	Calibration (1)	**Calibration (2)**	**Calibration (3)**	**Calibration (4)**	**Calibration (5)**
c(mm)	25.4847±6E-3	25.4028±1 E-3	25.4161±1.4E-2	25.4775±9E-3	25.4492±1E-2
x_P(mm)	3.1725±5E-3	3.1374±1E-3	3.1099±8E-3	3.1354±5E-3	3.1067±5E-3
y_p(mm)	2.4295±6.4E-4	2.4137±2E-3	2.4278±8.5E-4	2.4262±5.1E-4	2.4282±6.5E-4
K1	3.5E-4±1.9E-5	2. 92E-4±3.6E-5	5.55E-5±0	2.9E-4±1.3E-5	2.99E-4±1.5E-5
K2	-2.95E-5±1.6E-6	-2.75E-5±1.6E-6	0	-2.26E-5±9.3E-7	-1.66E-5±1E-6
K3	0	0	0	0	0
P1	0	0	0	0	0
P2	0	0	0	0	0
Image coverage (%)	83	80	80	83	83
Overall RMS (pixels)	0.368	0.333	0.3965	0.3606	0.3663
Δc(mm)	0.4847	0.4028	0.4161	0.4775	0.4492

Table (5.5): Calibration results of main parameters for camera SANYO (E1075), with fixed focal length (5.7mm).

	Calibration (1)	**Calibration (2)**	**Calibration (3)**	**Calibration (4)**	**Calibration (5)**
c(mm)	6.2017±5E-4	6.1929±1 E-3	6.1891±2E-3	6.2060±1E-3	6.2046±1E-3
x_P(mm)	2.9666±5E-4	2.9600±1E-3	2.9762±1E-3	2.9639±1E-3	2.9632±1 E-3
y_p(mm)	2.6588±6.1E-4	2.6768±2E-3	2.6665±2E-3	2.6722±2E-3	2.6484±1E-3
K1	4.22E-3±1.1E-5	4.23E-3±2.5E-5	4.27E-3±2.8E-5	4.26E-3±3.2E-5	4.31E-3±1.6E-5
K2	-3.98E-5±7.5E-7	-4.28E-5±2.3E-6	-5.38E-5±2.1E-6	-4.8E-5±2.6E-6	-5.14E-5±1.2E-6
K3	-5.23E-7±0	0	0	0	0
P1	-2.82E-4±4E-6	-1.69E-4±1.1E-5	-2.64E-4±9.8E-6	-2.09E-4±7.9E-6	-2.47E-4±8.2E-6
P2	4.97E-6±4.3E-6	8.91E-5±1.1E-5	2.2E-5±1.1E-5	6.59E-5±1.3E-5	-4.4E-5±9.6E-6
Image coverage (%)	90	80	87	83	92
Overall RMS (pixels)	0.2041	0.2407	0.2496	0.2375	0.2938
Δc(mm)	0.5017	0.4929	0.4891	0.5060	0.5046

Table (5.6): Calibration results of main parameters for camera SANYO (E1075), with fixed focal length (17.1mm).

	Calibration (1)	**Calibration (2)**	**Calibration (3)**	**Calibration (4)**	**Calibration (5)**
c(mm)	17.1272±2E-3	17.1270±4E-3	17.2058±2E-3	17.1178±3E-3	17.1285±3E-3
x_P(mm)	3.0101±3E-3	2.9955±8E-3	3.0091±2E-3	2.9822±4E-3	3.0921±5E-3
y_p(mm)	2.7049±4E-3	2.8044±6E-3	2.7024±3E-3	2.7149±6E-3	2.7244±6E-3
K1	2.22E-4±8.1E-6	2.29E-4±1.8E-5	2.46E-4±5.2E-6	2.17E-4±1.9E-6	2.28E-4±1.1E-5
K2	5.68E-6±6.3E-7	5.18E-6±1.2E-6	4.11E-6±3.1E-7	5.66E-6±5.5E-7	3.13E-6±7.3E-7
K3	-5.23E-7±0	0	0	0	0
P1	-1.7E-4±3.6E-6	-1.25E-4±8.8E-6	-1.42E-4±2.8E-6	-1.13E-4±4.6E-6	-1.52E-4±5.1E-6
P2	-9.79E-5±4.1E-6	0	-1.11E-4±2.9E-6	-9.11E-5±5.3E-6	-6.79E-5±5.8E-6
Image coverage (%)	88	86	80	89	89
Overall RMS (pixels)	0.1920	0.4491	0.1280	0.2206	0.2406
Δc(mm)	0.0272	0.0270	0.1058	0.0178	0.0285

In above tables, c is the focal length; **(x_p, y_p)** is the image center coordinates **;(k_1, k_2, k_3)**, **(p_1, p_2)** are the radial distortion and tangential distortion coefficients of the camera lens. According to PhotoModeler tutorial a value of RMS less than 1.0 pixel indicates a good calibration and very good calibrations can have a final total error smaller than 0.4 pixels [25]. In our cases, the most lab calibrations have a final total error less than 0.4 pixels.

In representing x_p, y_p and c from the previous data obtained by calibrating the readings recorded from cameras with various focal lengths in charts, as illustrated in figures below.

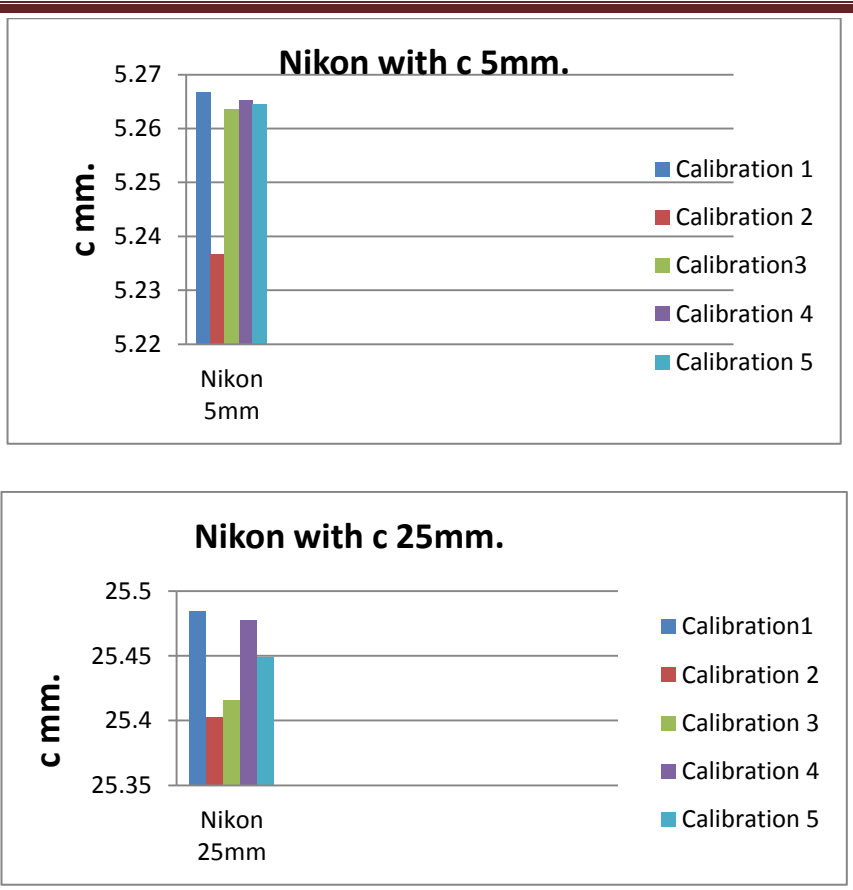

Figure (5.8): Comparison data of various focal lengths to the Nikon camera.

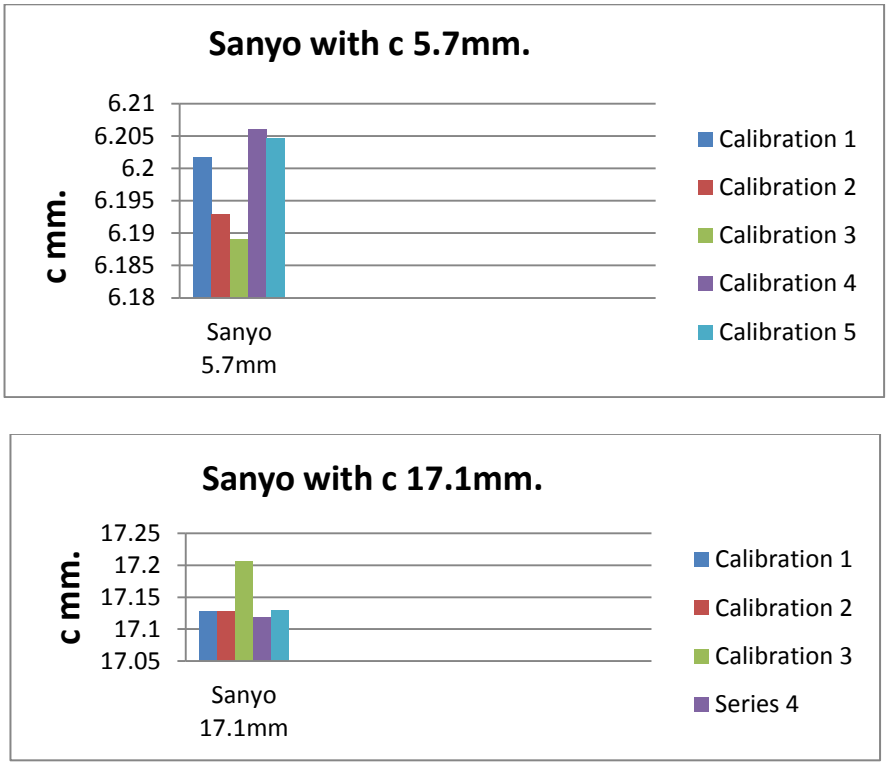

Figure (5.9): Comparison data of various focal lengths to the Sanyo camera.

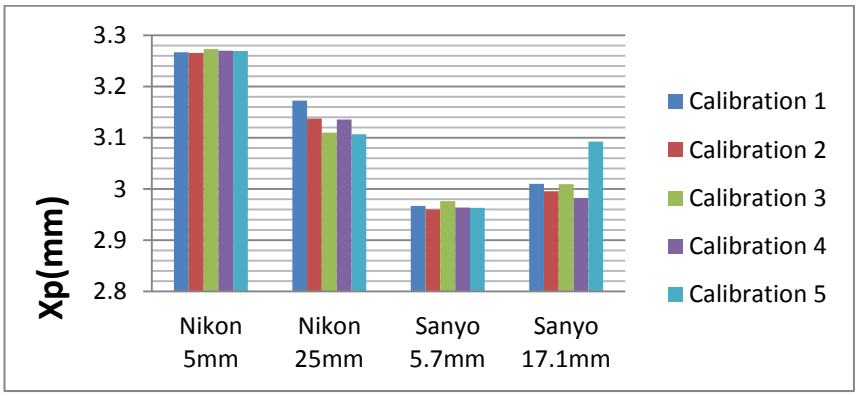

Figure (5.10): Comparison data of various x_p to cameras.

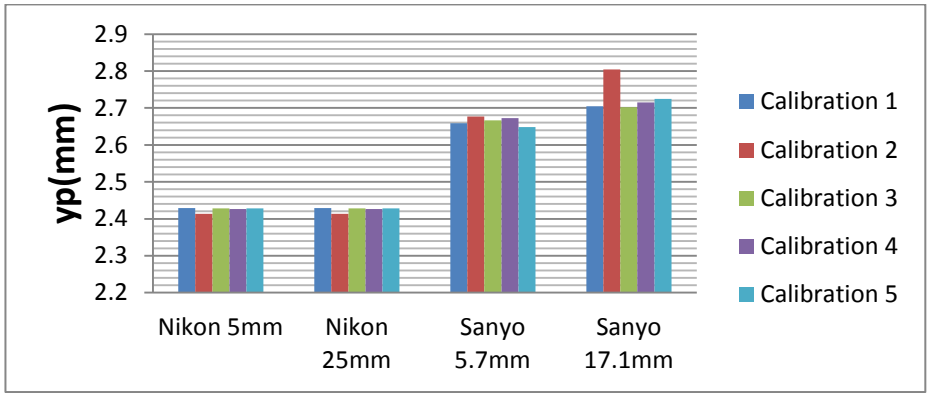

Figure (5.11): Comparison data of various y_p to cameras.

It is obtained that, undoubtedly, there is an error in x_p, y_p and c about (0.04) mm. observed during each reading with focal length (25 mm.). This error is great compared with the proposed accuracy from photogrammetry. For example, assume an object with distance (25 m.) far away from a camera station, its focal length (25 mm.), we get:

Using empirical formula $\text{Scale} = \frac{25}{25000} = \frac{1}{1000}$

So, we obtain that an error with 0. 04 mm. = 4 cm.

And there is an error in x_p, y_p and c about (0.02)mm. observed during each reading with focal length (5 mm), assume the distance (5m.) far away from camera station, its focal length (5mm.) given:

$$\text{Scale} = \frac{5}{5000} = \frac{1}{1000}$$

Therefore, we obtain that an error with 0.02 mm. = 2cm.

Therefore, without any doubt, calibration cannot be considered as constant or fixed for non-metric cameras, because such cameras have different (IOP) for each capture. Then the (IOP) must be evaluated in site for calibration matters. Any changes in the zoom of focus setting require new camera calibration.

5.5.4 Creating Dense Surface Model (DSM) Project

Dense Surface Modeling is a search algorithm that uses an existing pre-oriented project and pairs of photos from that project to search for image patches that look alike. This search is done in a regular grid-like manner, so a grid of 3D points is computed. When a good match is found between two photos, the orientation and camera data allow the program to compute the correct 3D location of the surface point corresponding to the image patch. With proper orientation and stereo overlap, a DSM or point cloud of 3D values can be created, edited, and converted to a triangulated mesh for export and advanced modeling and design. The basic steps of the DSM process are:

1. Start with an oriented, idealized, high-quality project with low residuals and at least two or more camera stations with suitable base-to-height ratios.

2. Define the extents of the search using Trim Tool to mark the area of interest on the images. It is possible to choose the area outside or inside the trim to create the 3D model.

3. The DSM algorithm first collects the pairs of photographs to be processed. Each pair of photographs overlaps is checked.

4. The algorithm searches along a row of the destination image using an NxN patch of imagery from the source image. Wherever it finds a good match it records it. The search range is controlled by the depth range parameters. The step size in the source image is defined by the sampling rate parameter. The sampling rate controls the distance between each point of the point mesh. The smaller value is set the longer time DSM processing takes, but the further point mesh can be generated and the quality increases by the increasing number of points. In this case, the sampling rate is set equal(1mm), by this value the number of the points mesh will be generated equals to (5563) points, these points are saved as a TXT file.

5. If more than one pair of photographs is being run, the results of each point cloud are then registered and merged into one cohesive point cloud.

6. The meshing steps and converting the point cloud into a triangulated mesh surface as in figure (5.12) below.

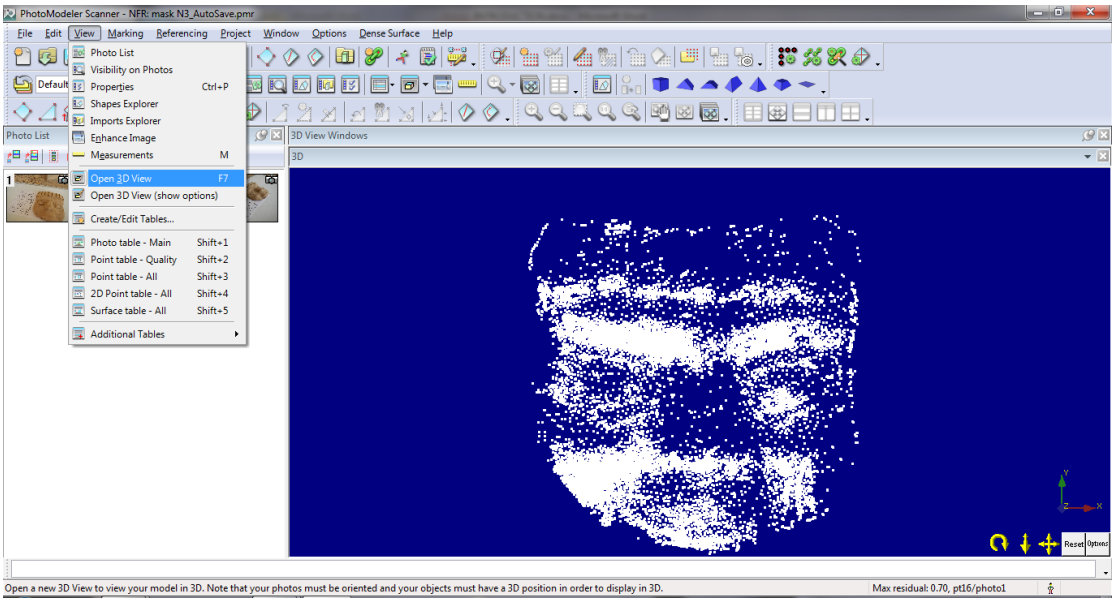

Figure (5.12): the 3D-points mesh.

7- A TXT file can be exported to many programs like AutoCAD or Surfer. It's exported to a surfer program to produce a contour model for the object, as in figure (5.13).

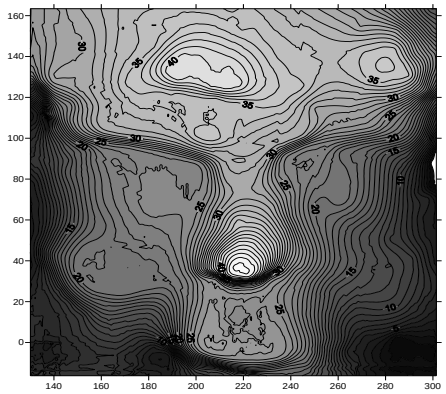

Figure (5.13): Derived contour map. The contour interval is 1.0mm.

The image pairs will be used to create the dense surface. It is necessary to choose a pair with a low angle between both images, suitable base-to-height ratio, low root mean square error (RMS), and small distance of the sampling rate, In this object the maximum residual equals to (o.70 pixel). By clicking Execute the point, mesh begins. The resulting 3D point

mesh can be viewed under the task View by clicking Open 3D View. Now a new window, which includes the generated point meshes showed up. In the 3D View Options dialogue box, Point Mesh has to be enabled as surface type to make the point cloud visible.

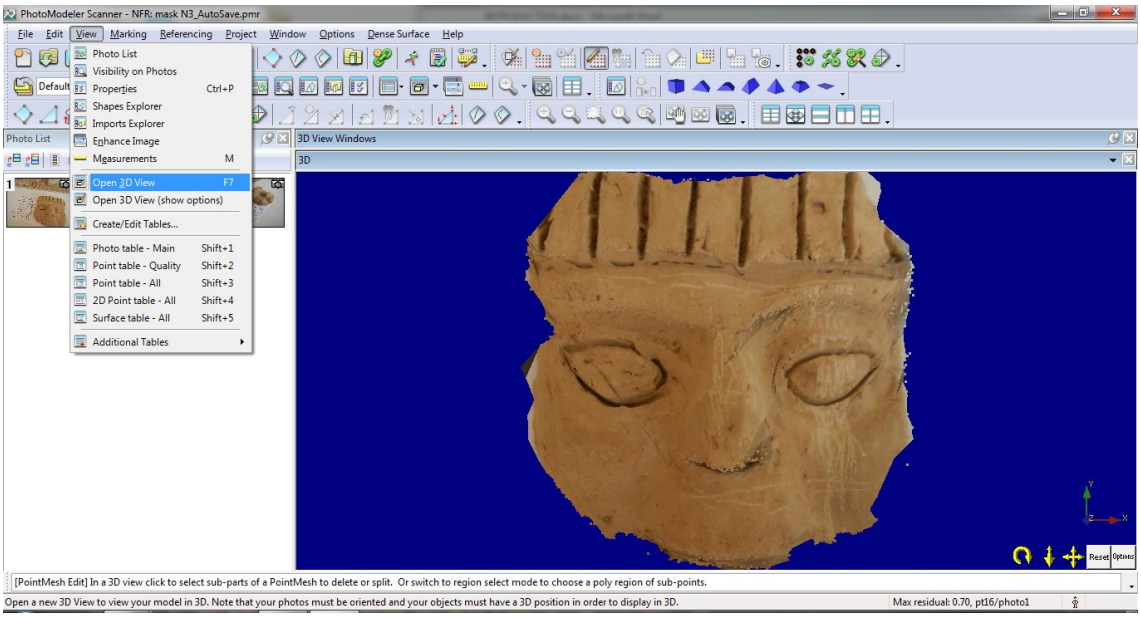

Figure (5.14): the 3D-point (stereomodel) with textures displayed in 3D-view.

Further, it is possible to change the display style into quality textures which visualizes the object with a more detailed surface by taking values from the source image (Figure 5.14). In the last step, the point cloud got meshed with triangulations between the points. Therefore, the point cloud got marked by clicking on it with the right click. Here it is possible to activate the triangulation. Now a certain surface has been generated which finally makes a proper 3D model out of the 3D point cloud. The coordinate points of the 3D point mesh are saved as a TXT file.

5.6 Using PhotoModeler as a Measurement Tool

One of the important current developments in digital close range photogrammetric systems are the full automation of the measuring process.

The very first step when starting an experimental model analysis project is the definition of the geometry used for visualization of the resulting mode shape. This geometry includes measurement points with a labeled and corresponding coordinates, and usually connections and surfaces allow a good visualization of the measured mode. When doing an experimental model analysis, one of the first tasks is the definition of the point to be measured, and to identify these points on the structures, then create a 3D model representing these measurement points. Two different scenarios are possible:

1. Comparison between the measurement of the points with targets and without targets (using small solid model).
2. Extract the accuracy of the represented 3D points from the façade of the building (using leas-square methods).

5.6.1 Measurement of the Points

The targets (points that are going to be measured) need to be marked. Mark is the process of creating and positioning an object on a photograph. This can either be done manually, by mouse-click on the appropriate location on the photograph or in an automated mode. For automated mode, circular targets with a high contrast background should be used. Therefore the points need to be referenced (at least six points each photo was selected). Referencing points is the process of telling the software that two points, marked on two different photographs, represent the same physical

point in space. The software will first calculate the relative camera positions, and then recalculate all the 3D coordinates of the points; by Photomodeler we can measure 3D coordinates of the points or the distance between any two points directly. Vernier used to check real distances between the points, see figure (5.15) below, the left photograph is without targets and the right photograph is with targets.

Figure (5.15): The photographs with targets and without targets.

The distance between points are presented in Table (5.7) measured by Vernier, Table (5.9) with targets and Table (5.10) without targets, respectively.

Table (5.7): Actual Distance (mm) by Vernier.

No	Measurement		Actual Distance (mm)
	From	To	
1	1	2	107.78
2	3	4	140.67
3	5	6	41.00
4	7	8	77.01

Table (5.8): The three coordinates of points by Photomodeler.

No. of point	X (mm.)	Y (mm.)	Z(mm.)
1	-294.005	108.353	69.155
2	-401.005	109.140	61.472
3	-273.151	50.313	33.175
4	-413.139	49.976	17.937
5	-304.630	50.009	24.021
6	-318.115	49.509	13.899
7	-319.980	46.606	6.702
8	-356.622	46.942	1.166

Table (5.9): The distance between points with targets.

No	**Measurement**		**Distance (mm)**
	From	**To**	
1	1	2	107.767
2	3	4	140.648
3	5	6	40.988
4	7	8	77.043

Table (5.10): The distance between points without targets.

No	**Measurement**		**Distance (mm)**
	From	**To**	
1	1	2	107.988
2	3	4	140.816
3	5	6	40.417
4	7	8	77.154

After measuring the distance between the points by Photomodeler with targets and without targets and compare with the actual distance by Vernier, the accuracy obtained from this results are ranges between (0.01 – 0.03) mm with target and ranges between (0.1 – 0.5) mm without targets, as in Table (5.11).

Table (5.11): The accuracy obtained from the Photomodeler

No	Measurement		Measurement with targets	Measurement without targets
	From	**To**	Absolute error (mm)	Absolute error (mm)
1	1	2	0.013	0.199
2	3	4	0.022	0.146
3	5	6	0.012	0.583
4	7	8	0.033	0.144

It is obtained that, from the above tables, and for the purpose of getting the proposed accuracy from photogrammetry by evaluating the three dimensions for the located points, such points should be well defined features by using targets.

5.6.2 Extract the Accuracy from the Presented Façade.

We can get a 3D points for any building by taking two or more photos and processing them by PhotoModeler to obtain a points cloud depending on the sampling rate located in the program as show in figure below:

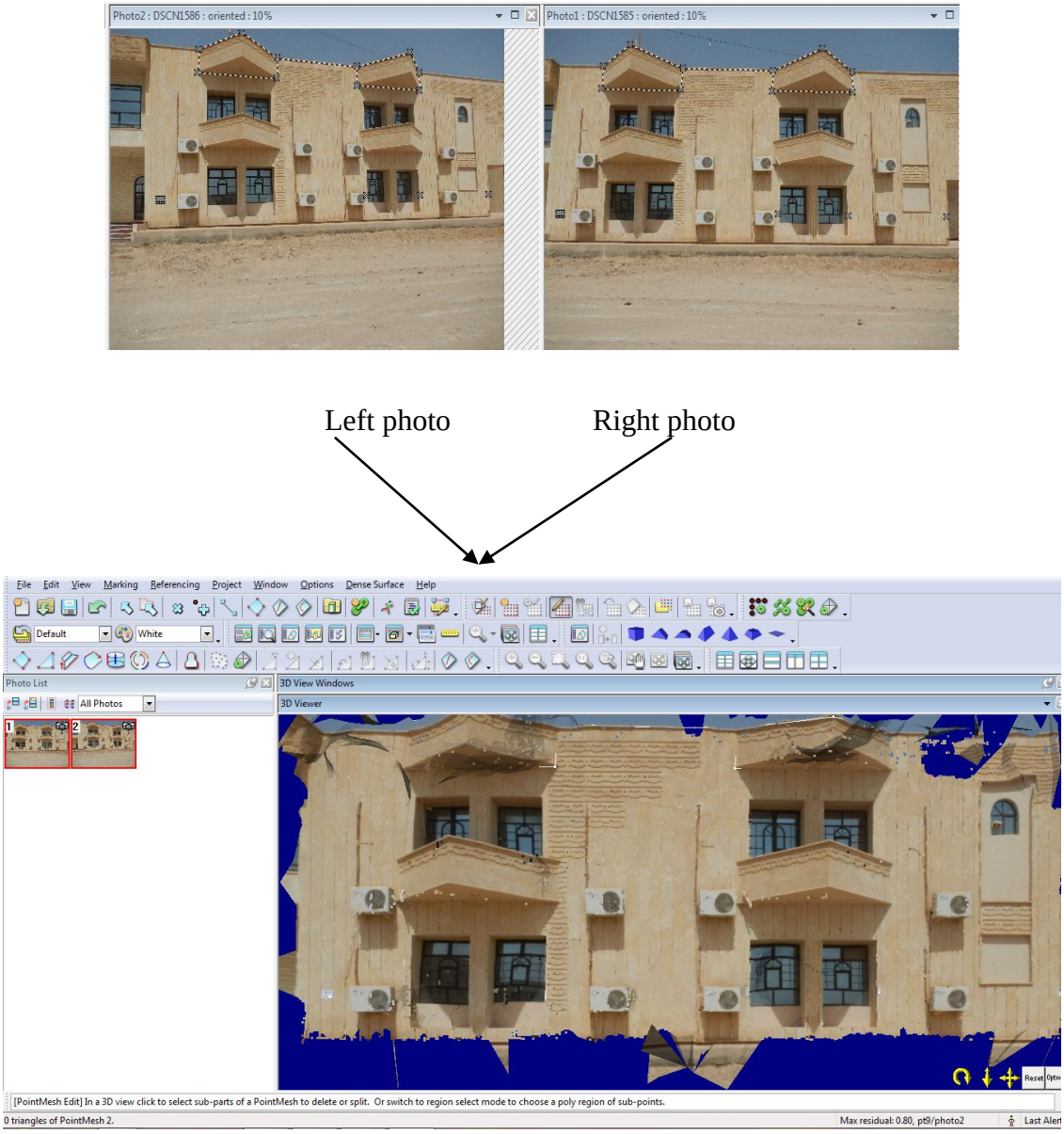

Figure (5.16): the 3D point's (stereomodel) of the building façade.

This building is represented by (53715) points and the sampling rate is (25 mm) computed automatically by the PhotoModeler and saved as txt file, with standard error for $\delta x = \pm 0.057\ mm$, $\delta y = \pm 0.11\ mm$ and $\delta z = \pm 0.33 mm$.The accuracy values are evaluated by (Least square method) presented in Appendix (B).

5.7 Illumination and object material

The main problems in this thesis can be described in the sub-section as follow:

1. Lighting

The lighting of the object and scene should also be considered. Usually it is not desirable to use a flash mounted on the camera because the shadows would move on the object between photos. Other similar light sources (including a bright sun) should not move between photographs. In the case of sunshine and outdoor scenes do not take photos hours or days apart, so that these types of lighting issues are minimized.

Avoid using lighting in the scene that causes glare, reflections or shadows on the surface. The glare/shadows on the surface can cause problems for the matching algorithm since the effects will appear in a different location in each photo and can be mistaken as part of the surface texture. This is especially true of shiny surfaces. Matt surfaces that do not show highlights from directed light sources are less prone to this problem and some side lighting and shadows are acceptable. Generally try to use flat light source such as the light outside on a cloudy day.

2. Surface Requirements

The surfaces to be modeled by dense point clouds need to have a visible random texture/pattern. Examples of random textures are rock, skin, wood grain, bricks, trees, etc. Examples of surfaces that are not textured are plaster-board walls, metal surfaces and glass windows. Some items may appear to be textured but the texture is consistently repeated and not random (certain cloth patterns, man-made objects like a window screen or a faux-leather pattern).

CHAPTER SIX
CONCLUSIONS AND RECOMMENDATIONS

6.1 Conclusions

Nowadays, both visual and scientific applications of 3D modeling are increasing day by day. 3D modeling products are used in many variety of disciplines. With the improving hardware and software 3D modeling studies can be done much more easily and faster. In this study, the role of digital close range photogrammetry in the obtaining of 3D model was investigated. It can be seen that, in the completed study from model, obtaining of the data with photogrammetry is quite accurate and fast.

From the obtained experimental results, the following conclusions have been made:

1. In order to get accurate and reliable results, must get a large number of multi-directional images.
2. There is no calibration for non-metric camera, simply because calibration means we have fixed values for (IOP) and they are unchangeable parameters.
3. To produce 3D models, needed object coordinates on the surface of the object can be obtain of in a short time and much more faster. Close range photogrammetry software and a consumer digital camera are sufficient for this works. All studies can be completed only using photographs. That is, this is a non-contact technology. For this reason,a photogrammetric method can be considered in risky places.

4. It also can be considered to survey directly immeasurable objects. This is the safest method from this point of view. One of the main features of photogrammetric methods is the short length of time required on site to carry out measurements. Office work during the evaluation stage is actually longer.
5. The surfaces to be modeled by dense point clouds need to have a visible random texture/pattern.
6. The lighting of the object and scene should also be considered. Usually it is not desirable to use a flash mounted on the camera because the shadows would move on the object between photos. Generally, try to use a flat light source such as the light outside on a cloudy day.
7. High accuracy obtained from this study (using a normal close range photogrammetry and PhotoModeler), this accuracy ranging from (10 - 30) microns, the measuring using coded targets.

6.2 Recommendations

1. It is recommended to monitor the historic buildings and the important antiques and observing the variations during time that happen upon them.
2. It is recommended to use Photomodeler with camera (DSLR) in close range photogrammetry
3. In this thesis used phtomodeler version 6, it is recommended to use close range photogrammetry with Photomodeler software version 7 there is new option known (automatic smart matching) this option was used without targets to create 3D models.

References:

1. Jose Luis Lerma and Antonio Garcia., (2004). **3D City Modelling and Visualization of Historic Centers**, Int workshop on vision techniques applied to the rehabilitation of city centers, 25-27 oct, Lisbon, Postugal.
2. Mila Koeva., (2004). **3D Realistic Modeling and Visualization of Buildings in Urban Areas**, Int sym on modern technologies, technologies, education and professional practice in geodesy and related fields, sofia, 04-05 Nov.
3. Ulrike Herbig and Peter Waldhausl., (1997). **Architectural photogrammetry information system**, ISPRS-International Archives of Photogrammetry and Remote Sensing, Volume XXXII, Part 5C1B.
4. Heuvel, F., (1998). **3D Reconstrution from a Single Image Using Geometric Constriants**, ISPRS Journal of Photogrammetry and Remote Sensing, No. 53, pp 345-368.
5. Gomes, J. M. G., (1999). **A Photogrammetry project in Brazil: The use of the Photomodeler Software**. http://cipa.icomos.org/fileadmin/papers/onlinda/99C3Bpdf.
6. Guidi G., and Tucci G., (2001). **Photogrammetry and 3D Scanning: Assessment of Metric Accuracy for the Digital Model of Danatello's Maddalena**, Padova, Italy. April 3-4. NRC 44879.
7. Lara L. O'Shields, and Tyler A. kress., (2004). **Determination and Verification of Equivalent Barrier Speed Using Photomodeler as a Measurement Tool**, Sae Technical Paper Series: Acident Reconstruction (SP-1873).
8. Chadler J. H., Fryer J. G., and Jack A., (2005). **Metric Capabilities of Low-Cost Digital Camera for Close Range Surface Measurement**, Photogrammetric Record, Mar. 2005, Vol. 20, Issue 109, pp 12-26.
9. Tommaselli, A., and Reiss, M., (2005). **A Photogrammetric Method for Single Image Orientation and Measurement**, Photgrammetric Engineering and Remote Sensing, Vol. 71, No. 6, pp 727-732.
10. Jauregui, D., (2006). **Photogrammetry Applications in Routine Bridge Inspection and Historic Bridge Documentation**, Transportation Research Record, No. 1958, pp. 24-32.
11. Arias, P., and Lorenzo, H., (2007). **Low-cost documentation of traditional agro-industrial building by close range photogrammetry**, Building and Environment, Vol. 42, pp.1817-1827.

12. Shashi M., and Kamal Jian., (2007). **Use of Photgrammetry in 3D Modeling and Visualization of Buildings**, Asian Research Publishing Network (ARPN). Vol. 2, No.2, April 2007.
13. Sakir Tasdemir and Murat Yakar., (2008). **Detemination of Body Measurement of a Cow by Image Analysis**, International Conference on Computer Systems and Technologies – ComSysTech'08.
14. Sofoodeh S. and A. Gruen., (2008). **Integration of Structured Ligt and Digital Camera Image Data for the 3D Reconstruction of an Ancient Globe**, The International Archives of the Photogrammetry, Remote Sensing and Spatial Information Sciences. Vol. XXXVII. Part B5. Beijing.
15. Hullo J. F. and Fares S., (2009). **Photogrammetry and Dense Stero Matching Approch Applied to the Documentation of the Cultural Heritage Site of Kilwa (Saudi Arabia)**, 22nd CIPA Symposium, October 11-15, Kyoto, Japan.
16. Salma, C. C., (1980). "**Manual of Photogrammetry**", 4th edition, American Society of photogrammetry.
17. Ghosh, Sanjib K., (1979). "**Analytical Photogrammetry**", Pergamon Press, New York.
18. Moffit, F. H. and Mikhail, E. M.,(1980). "**Photogrammetry**", 3th edition, Harper and Row Publishers, New York.
19. E. E.Derenyi., (1996)."**Photogrammetry : The Concepts**".
20. James R.Williamson,Ph.D., (2000)."**1 2 3 Photogrammetry**", InternetDocument, www.123photogrammetry.com/photogrammetry.html.
21. Wolf, P. R., (1983). "**Elements of Photogrammetry**", 2nd edition, McGraw Hill International Book Company.
22. Wolf, R., and Dewitt A., (2000). **Elements of Photogrammetry with Application in GIS**, 3rd edition.
23. ERDAS, Inc., (2008). ERDAS IMAGINE Version 9.3 **Leica Photogrammetry Suite Project Manager** User's Guide, USA.
24. Remondino, F., (2006). ***Image-Based Modeling or Object and Human Reconstruction***, Doctoral Thesis, Aristoteles University, Thessaloniki, Greece, Zurich. S. Ikeda, T. Sato, N. Yokoya, 2003, A calibration method for an omnidirectional multi-camera system, IS&T/SPIE's 15th Annual Symposium on Electronic Imaging, 20-24 January 2003, Santa Clara, California, USA
25. PhotoModeler Pro., (2008).**User Manual Eos System** Inc. Version 6.

26. Wilfried Linder, "Digital Photogrammetry", A Practical Courrse, 3rd edition. Germany, 2009.
27. Y. Do., S. H. Yoo, and D. S. Lee., (1998). **Direct Calibration Methodology for Stereo Camera**, SPIE Conf. vol . 3521: Machine vision systems for inspection and metrology VII, pp. 54-65.
28. William, K., (2004). **Digital Vertical Aerial Camera System for High Resolution Site Inspections in Conservation Easement Monitoring**. PhD Thesis. University of Maine. EEUU. Pp.26.
29. Atkinson, K. B., (2001). **Close Range photogrammetry and Machine Vision**. Scotland, UK: Whittles Publishing Company.
30. Boochs, F., A. Gehrhoff, and M. Neifer., (200). **An Object-Oriented Stereo System for 3D-Measurement**. IAPRS.XXXIII: 1-8.
31. Mikhail, E. M., S. J. Bethel, and J. C. McGlone., (2001). **Introduction to Modern Photogrammetry**. New York, USA: John Wiley&Sons, Inc.
32. Nikoon Coolpix AW100 (5-25) mm, Instruction Manual.
33. Sanyo VPC-E1075 (5.7-17.1) mm, Instruction Manual.
34. Thomas Luhmann & Stuart Robson, (2008). **Advances in Photogrammetry, Remote Sensing and Spatial Information Sciences**, ISPRS Congress Book 2008 Taylor & Francis Group, London, ISBN 978-0-415-47805-2,

Appendix (A)

Development and linearization of the collinearity condition equations

The collinearity condition equations are developed from similar triangles of fig. (2-9) as follows:-

$$\frac{x'}{X-XL}=\frac{y'}{Y-YL}=\frac{-z'}{Z-ZL}$$

Reducing,

$$x'=\left(\frac{X-XL}{Z-ZL}\right)z' \qquad \text{(a)}$$

$$y'=\left(\frac{Y-YL}{Z-ZL}\right)z' \qquad \text{(b)}$$

Also, by identifying

$$z'=\left(\frac{Z-ZL}{Z-ZL}\right)z' \qquad \text{(c)}$$

Any imaged point having coordinates x, y, and z in a tilted photo, which is determined as follows:-

$$\begin{aligned} x &= m_{11}x'+m_{12}y'+m_{13}z' \\ y &= m_{21}x'+m_{22}y'+m_{23}z' \\ z &= m_{31}x'+m_{32}y'+m_{33}z' \end{aligned} \qquad \text{…. (A-1)}$$

This equation described expressly in appendix (B)

Substituting (a), (b), and (c) into Eqs. (A-1)

$$x=m_{11}\left(\frac{X-XL}{Z-ZL}\right)z'+m_{12}\left(\frac{Y-YL}{Z-ZL}\right)z'+m_{12}\left(\frac{Z-ZL}{Z-ZL}\right)z' \qquad \text{…. (A-2)}$$

$$y=m_{21}\left(\frac{X-XL}{Z-ZL}\right)z'+m_{22}\left(\frac{Y-YL}{Z-ZL}\right)z'+m_{23}\left(\frac{Z-ZL}{Z-ZL}\right)z' \qquad \text{…. (A-3)}$$

$$z=m_{31}\left(\frac{X-XL}{Z-ZL}\right)z'+m_{32}\left(\frac{Y-YL}{Z-ZL}\right)z'+m_{33}\left(\frac{Z-ZL}{Z-ZL}\right)z' \qquad \text{…. (A-4)}$$

Factoring the term (z'/Z-ZL) from Eqs. (A-2) through (A-4), dividing (A-2) and (A-3) by (A-4), and substituting (- f) for (z), and adding corrections for offset of the principal point (x_0, y_0) the following collinearity equations results:

$$\begin{aligned} x &= x_0 - f\left[\frac{m_{11}(X-X_L)+m_{12}(Y-Y_L)+m_{13}(Z-Z_L)}{m_{31}(X-X_L)+m_{32}(Y-Y_L)+m_{33}(Z-Z_L)}\right] \\ y &= y_0 - f\left[\frac{m_{21}(X-X_L)+m_{22}(Y-Y_L)+m_{23}(Z-Z_L)}{m_{31}(X-X_L)+m_{32}(Y-Y_L)+m_{33}(Z-Z_L)}\right] \end{aligned} \qquad \text{…. (A-5)}$$

Where:-

(x_o, y_o) : Represent the principal point coordinates.

(x, y) : Represent the photo coordinates system.

(X, Y, Z) : Represent the ground coordinates system.

(X_L, Y_L, Z_L) : Represent the exposure station, coordinates in the ground coordinates system.

f : Is the calibrated camera focal length.

m's : Are functions of rotation angles omega (ω), phi (ϕ), and kappa (κ) and these are described expressly in appendix (B).

The Eqs. (A-5) are nonlinear with nine unknowns; three rotations angles (ω,ϕ,κ); three exposure station coordinates (X_L, Y_L, Z_L); and three object space coordinates (X,Y and Z), for each point. These non linear equations are linearized using Taylor's theorem. In linearizing the collinearity equations, Eqs. (A-5) are rewritten as follows:

$$F_1 = 0 = q \cdot x + r \cdot f$$
$$F_2 = 0 = q \cdot y + s \cdot f \qquad \text{…. (A-6)}$$

Where:-

$$q = m_{31}(X - X_L) + m_{32}(Y - Y_L) + m_{33}(Z - Z_L)$$
$$r = m_{11}(X - X_L) + m_{12}(Y - Y_L) + m_{13}(Z - Z_L)$$
$$s = m_{21}(X - X_L) + m_{22}(Y - Y_L) + m_{23}(Z - Z_L)$$

After applying Taylor's theorem for linearization, Eqs. (A-6) can be expressed as:-

$$0 = (F_1)_0 + \left(\frac{\partial F_1}{\partial x}\right)_0 dx + \left(\frac{\partial F_1}{\partial \omega}\right)_0 d\omega + \left(\frac{\partial F_1}{\partial \phi}\right)_0 d\phi + \left(\frac{\partial F_1}{\partial \kappa}\right)_0 d\kappa + \left(\frac{\partial F_1}{\partial X_L}\right)_0 dX_L + \left(\frac{\partial F_1}{\partial Y_L}\right)_0 dY_L + \left(\frac{\partial F_1}{\partial Z_L}\right)_0 dZ_L + \left(\frac{\partial F_1}{\partial X}\right)_0 dX + \left(\frac{\partial F_1}{\partial Y}\right)_0 dY + \left(\frac{\partial F_1}{\partial Z}\right)_0 dZ$$

$$0 = (F_2)_0 + \left(\frac{\partial F_2}{\partial y}\right)_0 dy + \left(\frac{\partial F_2}{\partial \omega}\right)_0 d\omega + \left(\frac{\partial F_2}{\partial \phi}\right)_0 d\phi + \left(\frac{\partial F_2}{\partial \kappa}\right)_0 d\kappa + \left(\frac{\partial F_2}{\partial X_L}\right)_0 dX_L + \left(\frac{\partial F_2}{\partial Y_L}\right)_0 dY_L + \left(\frac{\partial F_2}{\partial Z_L}\right)_0 dZ_L + \left(\frac{\partial F_2}{\partial X}\right)_0 dX + \left(\frac{\partial F_2}{\partial Y}\right)_0 dY + \left(\frac{\partial F_2}{\partial Z}\right)_0 dZ$$

Where:-

$(F_1)_0$ and $(F_2)_0$: Represent the Eqs. (A-6) evaluated using the approximate values of the unknowns.

$\left(\frac{\partial F_1}{\partial}\right) \& \left(\frac{\partial F_2}{\partial}\right)$: Represent the partial derivatives of the function (F_1) and (F_2) respectively.

dx, dy, dω, …, dZ : Represent small corrections to the unknowns to be computed.

Since (*dx* and *dy*) represent the corrections to the measured photo coordinates (*x, y*), they may be interpreted as residual errors in the measurements, so we can assume that (V_x=*dx*) and (V_y=*dy*). After substitution and simplification we obtained the following:-

$$V_x = b_{11}d\omega + b_{12}d\phi + b_{13}d\kappa - b_{14}dXL - b_{15}dYL - b_{16}dZL + b_{14}dX + b_{15}dY + b_{16}dZ + J \quad \text{…. (A-7)}$$

$$V_y = b_{21}d\omega + b_{22}d\phi + b_{23}d\kappa - b_{24}dXL - b_{25}dYL - b_{26}dZL + b_{24}dX + b_{25}dY + b_{26}dZ + K \quad \text{…. (A-8)}$$

Where:

$$b_{11} = \frac{f}{q^2}[r(-m_{33}\Delta Y + m_{32}\Delta Z) - q(-m_{13}\Delta Y + m_{12}\Delta Z)$$

$$b_{12} = \frac{f}{q^2}[\Delta X\cos\phi + \Delta Y(\sin\omega\cdot\sin\phi) + \Delta Z(-\sin\phi\cdot\cos\omega)] +$$

$$\frac{f}{q}[\Delta X(-\sin\phi\cdot\cos\kappa) + \Delta Y(\sin\omega\cdot\cos\phi\cdot\cos\kappa) + \Delta Z(-\cos\omega\cdot\cos\phi\cdot\cos\kappa)]$$

$$b_{13} = \frac{-f}{q}(m_{21}\cdot\Delta X + m_{22}\cdot\Delta Y + m_{23}\cdot\Delta Z)$$

$$b_{14} = \frac{rf}{q}(m_{31}) + \frac{rf}{q}(m_{11})$$

$$b_{15} = \frac{rf}{q^2}(m_{32}) - \frac{f}{q}(m_{12})$$

$$b_{16} = \frac{rf}{q^2}(m_{33}) - \frac{f}{q}(m_{13})$$

$$J = x_a - x_0 + \frac{rf}{q}$$

$$\Delta X = (X - X_L), \Delta Y = (Y - Y_L), \Delta Z = (Z - Z_L)$$

$$b_{21} = \frac{f}{q^2}[s(-m_{33}\Delta Y + m_{32}\Delta Z) - q(-m_{23}\Delta Y + m_{22}\Delta Z)]$$

$$b_{22} = \frac{f}{q^2}[\Delta X.\cos\phi + \Delta Y(\sin\omega.\sin\phi) + \Delta Z(-\cos\omega.\sin\phi)] +$$

$$\frac{f}{q}[\Delta X(\sin\phi.\sin\kappa) + \Delta Y(-\sin\omega.\cos\phi.\sin\kappa) + \Delta Z(\cos\omega.\cos\phi.\sin\kappa)]$$

$$b_{32} = \frac{f}{q}(m_{11}.\Delta X + m_{12}.\Delta Y + m_{13}.\Delta Z)$$

$$b_{24} = \frac{f}{q^2}(sm_{31} - qm_{21})$$

$$b_{25} = \frac{f}{q^2}(sm_{32} - qm_{22})$$

$$b_{26} = \frac{f}{q^2}(sm_{33} - qm_{23})$$

$$K = y_a - y_0 + \frac{sf}{q}$$

Appendix (B)

Development and linearization of the Three-dimensional conformal coordinate transformation equation

In figure (3-4) to convert a xyz to an XYZ, it requires the definition of seven parameters. These parameters are: its rotation angles omega (ω), phi (ϕ), and (κ); a scale factor (s); and three translation parameters T_X, T_Y, and T_Z. The transformation equations will be developed in the following two basic steps: (1) rotation and (2) scaling and translation.

As apparent in figure (3-4) with three steps to convert from xyz system to apply to x'y'z' system:

(1) Rotation through the angle ω about the x' axis is illustrated in figure (B-1). The coordinates of any point A in the once-rotated $x_1y_1z_1$ system, as shown graphically in figure (B-1), are

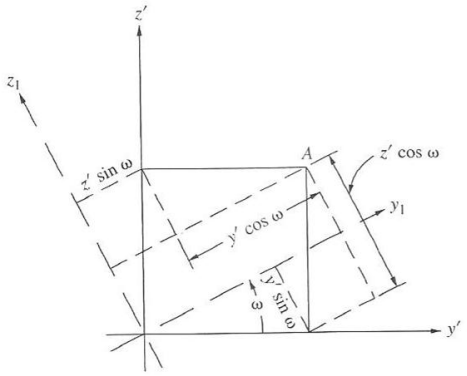

Figure (B-1) omega rotation about the x' axis.

$x_1 = x'$

$y_1 = y' \cos\omega + z' \sin\omega$ (B-1)

$z_1 = -y' \sin\omega + z' \cos\omega$

Since this rotation was about x', the x' and $x_1$axes are coincident and therefore the x coordinate of A is unchanged.

(2) Rotation through ϕ about they_1 axis is illustrated in figure (B-2). The coordinates of A in the twice-rotated$x_2y_2z_2$ coordinate system, as shown graphically in figure (B-2), are

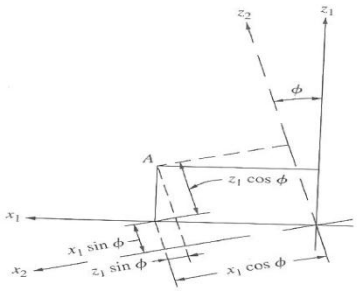

Figure (B-2) phi rotation about the$y_1$axis.

$$x_2 = -z_1 \sin\phi + x_1 \cos\phi$$

$$y_2 = y_1 \qquad \text{(B-2)}$$

$$z_2 = z_1 \cos\phi + x_1 \sin\phi$$

In this rotation abouty_1, the y_1 and y_2 axes are coincident, and therefore the y coordinate of A is unchanged. Substituting Eqs. (B-1) into Eqs. (B-2) gives

$$x_2 = -(-y'\sin\omega + z'\cos\omega)\sin\phi + x'\cos\phi$$

$$y_2 = y'\cos\omega + z'\sin\omega \qquad (B-3)$$

$$z_2 = (-y'\sin\omega + z'\cos\omega)\cos\phi + x_1\sin\phi$$

(3)Rotation through k about z_2, axis is illustrated in figure (B-3). The coordinate of A in three-times-rotated coordinate system, which has now become the *xyz* system as shown graphically in figure (B-3), are

$$x = x_2 \cos k + y_2 \sin k$$

$$y = -x_2 \sin k + y_2 \cos k \qquad \text{(B-4)}$$

$$z = z_2$$

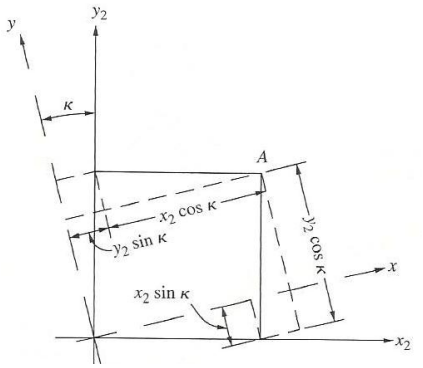

Figure (B-3) kappa rotation about z_2 axis.

In this rotation about z_2, the z_2 and z axes are coincident, and therefore the z coordinate of A is unchanged. Substituting Eqs. (B-3) into Eqs. (B-4) gives

$$x = \left[\left(y' \sin\omega - z' \cos\omega\right) \sin\emptyset + x' \cos\emptyset\right] \cos k + \left(y' \cos\omega + z' \sin\omega\right) \sin k$$

$$y = [(-y' \sin\omega + z' \cos\omega) \sin\emptyset - x' \cos\emptyset] \sin k$$

$$+\left(y' \cos\omega + z' \sin\omega\right) \cos k$$

$$z = (-y' \sin\omega + z' \cos\omega) \cos\emptyset + x' \sin\emptyset \qquad (B-5)$$

Factoring Eqs. (B-5) gives

$$x = x'(\cos\emptyset \cos k) + y'(\sin\omega \sin\emptyset \cos k + \cos\omega \sin k \quad + z'(-\cos\omega \sin\emptyset \cos k + \sin\omega \sin k)$$

$$y = x'(-\cos\emptyset \sin k) + y'(-\sin\omega \sin\emptyset \sin k + \cos\omega \cos k \quad + z'(\cos\omega \sin\emptyset \sin k + \sin\omega \cos k)$$

$$z = x'(\sin\emptyset) + y'(-\sin\omega \cos\emptyset) + z'(\cos\omega \cos\emptyset) \qquad (B-6)$$

Substituting m's for the coefficients of x', y', and z' in Eqs. (B-6) gives

$$x = m_{11}x' + m_{12}y' + m_{13}z'$$

$$y = m_{21}x' + m_{22}y' + m_{23}z'$$

$$z = m_{31}x' + m_{32}y' + m_{33}z' \qquad \text{B-3} \qquad (B-7)$$

Where

$$m_{11} = \cos\emptyset \cos k$$

$$m_{12} = \sin\omega \sin\emptyset \cos k + \sin\omega \sin k$$

$$m_{13} = -\cos\omega \sin\emptyset \cos k + \sin\omega \sin k$$

$$m_{21} = -\cos\emptyset \sin k$$

$$m_{22} = -\sin\omega \sin\emptyset \sin k + \cos\omega \cos k$$

$$m_{23} = \cos\omega \sin\emptyset \sin k + \sin\omega \cos k$$

$$m_{31} = \sin\emptyset$$

$$m_{32} = -\sin\omega \cos\emptyset$$

$$m_{33} = \cos\omega \cos\emptyset \qquad \text{(B-8)}$$

The rotation matrix is orthogonal matrix, which has the property that its inverse is equal to its transpose, eq. (B-7) may be rewritten, expressing x' y' z' coordinate in terms of x y z coordinates In expanded form this equations is:

$$x' = m_{11}x + m_{21}y + m_{31}z$$

$$y' = m_{12}x + m_{22}y + m_{32}$$

$$z' = m_{13}x + m_{23}y + m_{33}z \qquad \text{(B-10)}$$

2-Scaling and Translation

Multiply each of Eqs. (B-10) by a scale factor (*s*) and to add the translation factors T_X, $T_{Y,}$ and $T_{Z.}$

$$X = sx' + T_X = s(m_{11}x + m_{21}y + m_{31}z) + T_X$$

$$Y = sy' + T_Y = s(m_{12}x + m_{22}y + m_{32}z) + T_Y$$
$$Z = sx' + T_Z = s(m_{13}x + m_{23}y + m_{33}z) + T_Z \qquad \text{(B-11)}$$

These non linear equations are linearized using Taylor's theorem. In linearizing the three-dimensional conformal coordinate translation equations, Eqs. (B-11) are rewritten as follows:

$$X_P = (X_P)_0 + (\frac{\partial X_P}{\partial s})_0 ds + (\frac{\partial X_P}{\partial \omega})_0 d\omega + (\frac{\partial X_P}{\partial \emptyset})_0 d\emptyset + (\frac{\partial X_P}{\partial k})_0 dk + (\frac{\partial X_P}{\partial T_X})_0 dT_X + (\frac{\partial X_P}{\partial T_Y})_0 dT_Y + (\frac{\partial X_P}{\partial T_Z})_0 dT_Z$$

$$Y_P = (Y_P)_0 + \left(\frac{\partial Y_P}{\partial s}\right)_0 ds + \left(\frac{\partial Y_P}{\partial \omega}\right)_0 d\omega + \left(\frac{\partial Y_P}{\partial \emptyset}\right)_0 d\emptyset + \left(\frac{\partial Y_P}{\partial k}\right)_0 dk + \left(\frac{\partial Y_P}{\partial T_X}\right)_0 dT_X + (\frac{\partial Y_P}{\partial T_Y})_0 dT_Y + (\frac{\partial Y_P}{\partial T_Z})_0 dT_Z \qquad \text{(B-12)}$$

$$Z_P = (Z_P)_0 + (\frac{\partial Z_P}{\partial s})_0 ds + (\frac{\partial Z_P}{\partial \omega})_0 d\omega + (\frac{\partial Z_P}{\partial \emptyset})_0 d\emptyset + (\frac{\partial Z_P}{\partial k})_0 dk + (\frac{\partial Z_P}{\partial T_X})_0 dT_X + (\frac{\partial Z_P}{\partial T_Y})_0 dT_Y + (\frac{\partial Z_P}{\partial T_Z})_0 dT_Z$$

In Eqs.(B-12), $(X_P)_0$, $(Y_P)_0, and (Z_P)_0$ are right-hand sides of Eqs. (B-10),$\left(\frac{\partial X_P}{\partial s}\right)_0$, $(\frac{\partial X_P}{\partial \omega})_0$, etc., are the partial derivatives with respect to the indicated unknown evaluated at the initial approximations, and $ds, d\omega, d\emptyset, dk, dT_X, dT_Y, and\ dT_Z$ are corrections to the initial approximations which will be computed during the solution.

Substituting letters for partial derivative coefficients, adding residuals to make the equations suitable for a least squares solution, and rearranging terms, the following equations result.

$$a_{11}ds + a_{12}d\omega + a_{13}d\emptyset + a_{14}dk + a_{15}dT_X + a_{16}dT_Y + a_{17}dT_Z = [X_P - (X_P)_0 + \gamma_{XP}$$

$$a_{21}ds + a_{22}d\omega + a_{23}d\emptyset + a_{24}dk + a_{25}dT_X + a_{26}dT_Y + a_{27}dT_Z = [Y_P - (Y_P)_0 + \gamma_{YP}$$

$$a_{31}ds + a_{32}d\omega + a_{33}d\emptyset + a_{34}dk + a_{35}dT_X + a_{36}dT_Y + a_{37}dT_Z$$

$$= [Z_P - (Z_P)_0 + \gamma_{ZP} \quad \text{(B-14)}$$

Where:

$a_{11} = m_{11}x_P + m_{21}y_P + m_{31}z_P$

$a_{12} = 0$

$a_{13} = [(-\sin\emptyset\cos k)x_P + \sin\emptyset\cos k\,(y_P) + \cos\emptyset\,(z_P)]s$

$a_{14} = (m_{21}x_P - m_{11}y_P)s$

$a_{15} = a_{26} = a_{37} = 1$

$a_{16} = a_{17} = a_{25} = a_{27} = a_{35} = a_{36} = 0$

$a_{21} = m_{12}x_P + m_{22}y_P + m_{32}z_P$

$a_{22} = (-m_{13}x_P - m_{23}y_P - m_{33}z_P)s$

$a_{23} = [(\sin\omega\cos\emptyset\cos\emptyset k)x_P + (-\sin\omega\cos\emptyset\sin k)(y_P) + (\sin\omega\sin\emptyset)(z_P)]s$

$a_{24} = (m_{22}x_P - m_{12}y_P)s$

$a_{31} = m_{13}x_P + m_{23}y_P + m_{33}z_P$

$a_{32} = (m_{12}x_P + m_{22}y_P + m_{32}z_P)s$

$a_{33} = [(-\cos\omega\cos\emptyset\cos\emptyset k)x_P + (\cos\omega\cos\emptyset\sin k)y_P + (-\cos\omega\sin\emptyset)z_P)]s$

$a_{34} = (m_{23}x_P - m_{13}y_P)$

Appendix (C):

Technical data of digital camera chips

Chip size (nominal)	Diagonal (mm)	Width (mm)	Height (mm)	No. of pixel	Pixel size (µm)
1/3.6"	5.0	4.0	3.0	1280×960	3.2
1/3.2"	5.7	4.0	3.4	1620×1220	2.8
1/3"	6.0	4.8	3.6		
1/2.7"	6.6	5.3	4.0	2048×1536	2.6
1/2.5"	7.1	5.7	4.2	2288×1712	2.5
1/2.4"	7.4	5.9	4.4	2592×1944	2.3
1/2"	8.0	6.4	4.8	1280×1024	6.0
				1280×1024	5.0
1/1.8"	8.93	7.2	5.3	2048×1536	3.45
				2080×1542	3.45
				2592×1944	2.8
				2272×1704	3.1
1/1.7"	9.5	7.6	5.6	2048×1536	3.7
2/3"	11	8.8	6.6	2560×1920	3.4
	11	8.8	6.6	3264×2448	2.6
1"	16	12.8	9.6		
4/3"	22/5	18.0	13.5	2614×1966	6.8
	21.8	17.4	13.1	2560×1920	6.8
		20.7	13.8	2268×1512	9.13
	27.3	22.7	15.1	3072×2048	7.4
	42.6	35.8	23.1	4064×2704	8.8
		36	24	4536×3024	7.9
	34.5	28.7	19.1	2464×1648	11.6

See the camera's manual for the nominal chip size (say 1/2.7") and the resolution, then use the table to find the pixel size. If the manual instead of the nominal chip size the border lengths (width and heght in mm) of the chip are given you can directly calculate the pixel size:

$$Pixel\ size\ (\mu m) = \frac{width \times 1000}{No.of\ columns} = \frac{height \times 1000}{No.\ of\ rows}$$

Appendix (D)

Excetract the Accuracy of Points from Presented Façade.

Computing the standard error **(**δx, δy, and δz) for the points (1 ,2, 3) in figure below, the coordinates of these points measured by photomodeler. Applying least square method to compute the standard error of the points.

In figure below, three points were measured by photomodeler, four times each one. Applying the least square method to determine the residual v (error in measurement) and standard error δ for the x,y,z to each point.

Point no. (1)	X (m)	Y(m)	Z(M)
1	10.918652	0.0767367	0.885369
2	10.918641	0.0767402	0.884052
3	10.918648	0.077392	0.887465
4	10.918660	0.077359	0.887465

By least square method:

$AX - L = v_1$

$X = x_1 \rightarrow X = x_1 + v_1 \rightarrow X - x_1 = v_1$

$X = x_2 \rightarrow X = x_2 + v_2 \rightarrow X - x_2 = v_2$

$X = x_3 \rightarrow X = x_3 + v_3 \rightarrow X - x_3 = v_3$

$X = x_4 \rightarrow X = x_4 + v_4 \rightarrow X - x_4 = v_4$

$$\begin{bmatrix}1\\1\\1\\1\end{bmatrix}[X]-\begin{bmatrix}x_1\\x_2\\x_3\\x_4\end{bmatrix}=\begin{bmatrix}v_1\\v_2\\v_3\\v_4\end{bmatrix}$$

Normal equation NX= D $\rightarrow$ $N=A^TA$

$$N=[1\quad 1\quad 1\quad 1]\begin{bmatrix}1\\1\\1\\1\end{bmatrix}=[4]$$

$$D=A^TL=[1\quad 1\quad 1\quad 1]\begin{bmatrix}x_1\\x_2\\x_3\\x_4\end{bmatrix}=[x_1+\quad x_2+\quad x_3+\quad x_4]$$

NX= D $\rightarrow$ $[4][X]=[x_1+\quad x_2+\quad x_3+\quad x_4]$

X= $N^{-1}D$ $\rightarrow N^{-1}=\frac{1}{4}\rightarrow$ $X=\frac{x_1+\quad x_2+\quad x_3+\quad x_4}{4}$

X= $\frac{43.674601}{4}=10.918650\,m.$ $its\ means$:

$$\begin{bmatrix}v_1\\v_2\\v_3\\v_4\end{bmatrix}=\begin{bmatrix}1\\1\\1\\1\end{bmatrix}[10.91865025]-\begin{bmatrix}10.918652\\10.918641\\10.918648\\10.918660\end{bmatrix}=\begin{bmatrix}-1.75\times10^{-6}\\9.25\times10^{-6}\\2.25\times10^{-6}\\-9.75\times10^{-6}\end{bmatrix}$$

$$\delta=\sqrt{\frac{\varepsilon v^2}{n-1}}=\sqrt{\frac{\varepsilon v^2}{4-1}}=7.932\times10^{-6}$$

$$\delta x=\mp\frac{\delta}{\sqrt{n}}=\mp3.966\times10^{-6}\,m.\ \approx\mp4\,micron$$

In the same way, compute $\delta y and\ \delta z$ to the same point

$\delta y = 1.84025 \times 10^{-4} \approx \mp 0.1mm$

$\delta z = 8.605 \times 10^{-4} \approx \mp 0.8mm$

To compute δx, δy, and δz for two points (2,3) in figure above, the coordinates of these points illustrated in tables below.

Point no. (2)	X (m)	Y(m)	Z(M)
1	14.396505	0.018325	1.154881
2	14.396780	0.018574	1.154901
3	14.396523	0.018443	1.154703
4	14.396932	0.018178	1.154218

By the same way, we compute:

δx= $\mp 1.0355 \times 10^{-4} m \approx 0.1\ mm.$

$\delta y = \mp 1.79097 \times 10^{-4} m \approx 0.17\ mm.$

$and\ \delta z = \mp 1.5894 \times 10^{-4} m \approx 0.15\ mm.$

Point no. (3)	X (m)	Y(m)	Z(M)
1	19.297108	0.006454	1.505534
2	19.297179	0.006676	1.505662
3	19.297401	0.006296	1.505586
4	19.297130	0.006407	1.505461

By the same way, computed:

δx= $\mp 6.71596 \times 10^{-5} m \approx 0.067\ mm.$

$\delta y = \mp 7.978343 \times 10^{-5} m \approx 0.08\ mm.$

$and\ \delta z = \mp 4.238319 \times 10^{-5} m \approx 0.04\ mm.$

$Therefor\ the\ standard\ error\ for\ all\ points$:

$\delta x = \mp 0.057mm.$

$\delta y = \mp 0.11mm.$

$\delta z = \mp 0.33mm.$

الخلاصة

ان مصدر البيانات الاساسي للنماذج ثلاثية الابعاد وللأجسام ذات السطوح النظامية و الغير نظامية يعرف ب (أو يحسب على اساس انه) احداثيات نقطة. ان الحصول على نموذج ثلاثي الابعاد للأجسام ذات السطوح الغير نظامية يحتاج نقاط كثيرة لتمثيل ذلك الجسم او السطح بدقة عالية. هذه النقاط يمكن ان نحصل عليها بسهولة بالطرق التقليدية وطرق المسح التصويري. في دراستنا هذه، الحالة والقابلية للمسح التصويري قريب المدى قد تم التحري عنها من اجل الحصول على نموذج ثلاثي الابعاد(3D). لذلك الاجسام ذات السطوح الغير نظامية قد أستخدمت لتقييم قدرة طرق المسح التصويري، حيث تم اخذ صور للأجسام طبقآ لمتطلبات المسح التصويري.

هذه الدراسة، تمت على ثلاثة مراحل، المرحلة الاولى هو معايرة الكاميرات المستخدمة حيث تم استخدام كامرتين هما ,(NIKOON COOLPIX AW100), و(SANYO E1075) وهي ذات قدرة تميزية وبعد بؤري يختلف في كلا الكاميرتين حيث تمت معايرة الكامرتين ببعدين بؤريين مختلفين مختبريآ وبواقع خمسة مرات لكل بعد بؤري في كل كاميرة .وتم الحصول على نتائج متغيرة وغير ثابتة لعوامل التوجيه الداخلي اي انه كا ن هناك فرق في اهم العوامل البعد البؤري (c) واحداثيات مركز الصورة (x_p , y_p) مقداره يتراوح من 0.02 mm الى.mm ٠.٠٤ وهذا الفرق كبير قياسآ بالدقة المتوخاة من المسح التصويري. لذلك، للحصول على دقة عالية من المسح التصويري ذو المدى القريب يجب مراعاة عمل المعايرة للكاميرة حقليآ اثناء العمل ودون اطفاء الكاميرة .المرحلة الثانية هو انتاج جسم ثلاثي الابعاد وبنقاط كثيفة جدآ اعتماداً على المسافة

(Sampling rate) بين نقطة واخرى من خلال عدة لقطات أثنان او اكثر يتم انتاج جسم ثلاثي الابعاد وبدقة عالية، في هذه الحالة تم استخدام جسم على شكل وجه مصنوع من الطين حيث تم تشكيل جسم ثلاثي الابعاد وبحوالي (٣٦٥٥) نقطة ثلاثية الابعاد وبمسافة(١) مليمتر بين نقطة واخرى،حيث انه كلما كانت نسبة الاعتيان قليلة كانت عملية المعالجة اطول والنقاط اكثر. من هذه العملية يمكن الاستفادة من توثيق التراث الثقافي والتاريخي للبلد في مكتبة رقمية تحفظ التحف النادرة ويمكن مراقبة هذه الاجسام من خلال هذه المكتبة وما يحدث على هذه التحف من تغير بمرور الزمن. المرحلة الثالثة والاخيرة تم استعمال برنامج (Photomodeler Scanner version 6) كأداة للقياس حيث استخدم في هذه المرحلة نموذج صغير على شكل بيت وتم القياس على اركان البيت حيث تم القياس بأسلوبين،ألاسلوب الاولى استخدمت الاهداف المشفرة التي يتعرف عليها البرنامج اتوماتيكيآ وتم تثبيت هذه الاهداف على اركان النموذج وكانت دقة القياس عالية جدآ تتراوح من ١٠ الى ٣٠ مايكروميتر .ألاسلوب الثاني من خلال القياس بدون اهداف مشفرة وانما الاعتماد على تطابق اركان النموذج في الصور وتكوين نقاط ثلاثية الابعاد منها يتم قياس المسافة بين ركن واخر وكانت الدقة جيدة تراوحت بين ٠.١ الى ٠.٥ مليمتر . برنامج (Photomodeler Scanner version 6) يحتاج أن يُدخلة له اي مسافة معلومة بين نقطتين على الجسم، وبعد ذلك البرنامج يقوم بحساب الاحداثيات ثلاثية الابعاد لأي نقطة على الجسم.

ثم بعد ذلك اخذت صور لبناية تقع في جامعة بابل على بعد ٢٥ متر(مسافة الالتقاط) ومن الصورتين تم تمثيل البناية كنموذج ثلاثي الابعاد بعدد هائل من النقاط بلغ (53715) نقطة وكان الخطا المعياري لهذه النقاط في كل من $\delta x=\mp 0.057mm.$ ، $\delta y=\mp 0.11mm..$ ، $\delta z=\mp 0.33mm.$.

جمهورية العراق
وزارة التعليم العالي والبحث العلمي
الجامعة التكنولوجية
قسم هندسة البناء والانشاءات

انشاء نموذج ثلاثي الابعاد بأستخدام كاميرا رقمية غير مترية في المسح التصويري ذي المدى القريب

رسالة مقدمة الى قسم هندسة البناء والانشاءات في الجامعة التكنولوجية
و هي جزءً من متطلبات نيل درجة الماجستير في علوم هندسة البناء والانشاءات
(هندسة الجيوماتيك)

من قبل
أيسر جميل الجنابي

باشراف
أ.م. د.عباس زيدان خلف
م.د. مزاحم عبد الكريم علوان

٢٠١٢